J. metamorphic Geol., 2006, **24,** 409–428 doi:10.1111/j.1525-1314.2006.00645.x

Albite vein formation during exhumation of high-pressure terranes: a case study from alpine Corsica

J. A. MILLER[1] AND I. CARTWRIGHT[2]
[1]*Department of Geology, University of Stellenbosch, Private Bag X1, Matieland 7602, South Africa (jmiller@sun.ac.za)*
[2]*School of Earth Sciences, Monash University, Melbourne, Vic. 3800, Australia*

ABSTRACT The formation of late-stage veins can yield valuable information about the movement and composition of fluids during uplift and exhumation of high-pressure terranes. Albite veins are especially suited to this purpose because they are ubiquitously associated with the greenschist facies overprint in high-pressure rocks. Albite veins in retrogressed metabasic rocks from high-pressure ophiolitic units of Alpine Corsica (France) are nearly monomineralic, and have distinct alteration haloes composed of actinolite + epidote + chlorite + albite. Estimated *P–T* conditions of albite vein formation are 478 ± 31 °C and 0.37 ± 0.14 GPa. The *P–T* estimates and petrographic constraints indicate that the albite veins formed after the regional greenschist facies retrogression, in response to continued decompression and exhumation of the terrane. Stable isotope geochemistry of the albite veins, their associated alteration haloes and unaltered hostrocks indicates that the vein-forming fluid was derived from the ophiolite units and probably from the metabasalts within each ophiolite slice. That the vein-forming fluid was locally derived means that a viable source of fluid to form the veins was retained in the rocks during high-pressure metamorphism, indicating that the rocks did not completely dehydrate. This conclusion is supported by the observation of abundant lawsonite at the highest metamorphic grades. Fluids were liberated during retrogression via decompression dehydration reactions such as those that break down hydrous high-pressure minerals like lawsonite. Albite precipitation into veins is sensitive to the solubility and speciation of Al, which is more pressure sensitive than other factors which might influence albite vein formation such as silica saturation or Na:K fluid ratios. Hydraulic fracturing in response to fluid generation during decompression was probably the main mechanism of vein formation. The associated pressure decrease with fracturing and fluid decompression may also have been sufficient to change the solubility of Al and drive albite precipitation in fracture systems.

Key words: albite veins; Corsica; exhumation; fluids; ophiolite; retrogression.

INTRODUCTION

Veins are one of the most visible manifestations of fluid flow. A large number of studies have focussed on utilizing the chemical, thermal and structural information that can be obtained from the study of veins to assess the degree of coupling between deformation, metamorphism and fluid flow (e.g. Yardley, 1983; Selverstone *et al.*, 1991, 1992; Bebout & Barton, 1993; Oliver, 1996; van der Klauw *et al.*, 1997; Agard *et al.*, 2000; Cartwright & Buick, 2000; Bons, 2001). This type of information can potentially help to constrain larger crustal-scale processes such as the initiation and propagation of faults and shear zones, partial melting processes at different levels in the crust and density changes in rocks during compaction and burial.

In general, veins represent complex geochemical systems whose character is dependent on a wide range of variables including: (1) the pressure and temperature of vein formation; (2) the chemistry of the vein-forming fluid; (3) the volume of fluid; (4) the scale of chemical transport; and (5) the mechanism of vein formation. In recent years two broad models of vein formation have been proposed. The first model, based largely on theoretical modelling has suggested that veins are the products of large-scale fluid flow systems (e.g. Wood & Walther, 1986; Ferry & Dipple, 1991; Bebout & Barton, 1993). The second model, based more on field and analytical data has suggested that veins are the products of small-scale fluid transport (Yardley & Bottrell, 1992; Slater *et al.*, 1994; Henry *et al.*, 1996; Cartwright & Barnicoat, 1999). In terms of the presence of veins in high-pressure metamorphic rocks, the later model has generally been favoured (e.g. Philippot & Selverstone, 1991; Getty & Selverstone, 1994). However, in general, the retrogression of high-pressure rocks is commonly associated with extensive veining that reflects the mobility of fluids during exhumation (Barnicoat, 1988; Bebout & Barton, 1989; Thomas, 1990, 1991; Barrientos, 1991; Philippot & Selverstone, 1991; Selverstone *et al.*, 1992; van der

Klauw *et al*., 1997; Miller *et al*., 1998; Cartwright & Buick, 2000).

Whilst a variety of vein types occur in high-pressure terranes, including quartz, omphacite, garnet, glaucophane, aluminosilicate and calcite veins (Agard *et al*., 2000; Brunsmann *et al*., 2000; Philippot & Rumble, 2000), albite veins are potentially the most useful for understanding fluid processes during exhumation. This is because, unlike quartz and calcite veins that may form at high pressures (Kerrich, 1988; Nelson, 1991; Cartwright & Barnicoat, 1999), albite veins in metabasic rocks are ubiquitously associated with extensive greenschist facies retrogression that unambiguously ties their formation to exhumation. This study examines the formation of albite veins in metabasic rocks from the high-pressure ophiolitic units from Alpine Corsica (France). The two principal aims of this study are to: (1) assess the chemical controls on albite vein formation, including fluid sources, volumes and compositions; and (2) to postulate a model for the formation of albite veins in high-pressure terranes.

GEOLOGICAL SETTING

The island of Corsica (Fig. 1) is dominated by Hercynian granitic basement in the south-west and an ophiolite-bearing high-pressure Alpine complex in the north-east. The Corsican ophiolite (Fig. 1) represents remnant Jurassic Piemontese-Ligurian (Tethyan) ocean crust, destroyed during the Alpine Orogeny. In general, the ophiolite underwent high-pressure metamorphism in response to intra-oceanic subduction associated with the convergence of the European continental margin and the Apulia microplate (Warburton, 1986; Coward & Dietrich, 1989; Waters, 1990; Pognante, 1991; Malavielle *et al*., 1998). The high-pressure metamorphism on Corsica has been dated at 85 Ma using Sm–Nd geochronology (Lahondère & Guerrot, 1997). However, this age may need to be revised in light of the much younger ages (Eocene) obtained using SHRIMP U–Pb and Sm–Nd geochronology elsewhere in the western Alps (Bowtell *et al*., 1994; Cliff *et al*., 1997; Rubatto *et al*., 1998).

Alpine Corsica

Alpine Corsica is composed of ophiolitic thrust slices inter-leaved with metasedimentary rocks within two different nappe stacks (Fig. 1). The lower nappe stack, the Schistes Lustrès Inférieur, is composed of several generally east-dipping thrust slices, all of which record the effects of high-pressure Alpine metamorphism, although *P–T* conditions are variable (Caron, 1994). Minimum *P–T* conditions for the eclogite facies

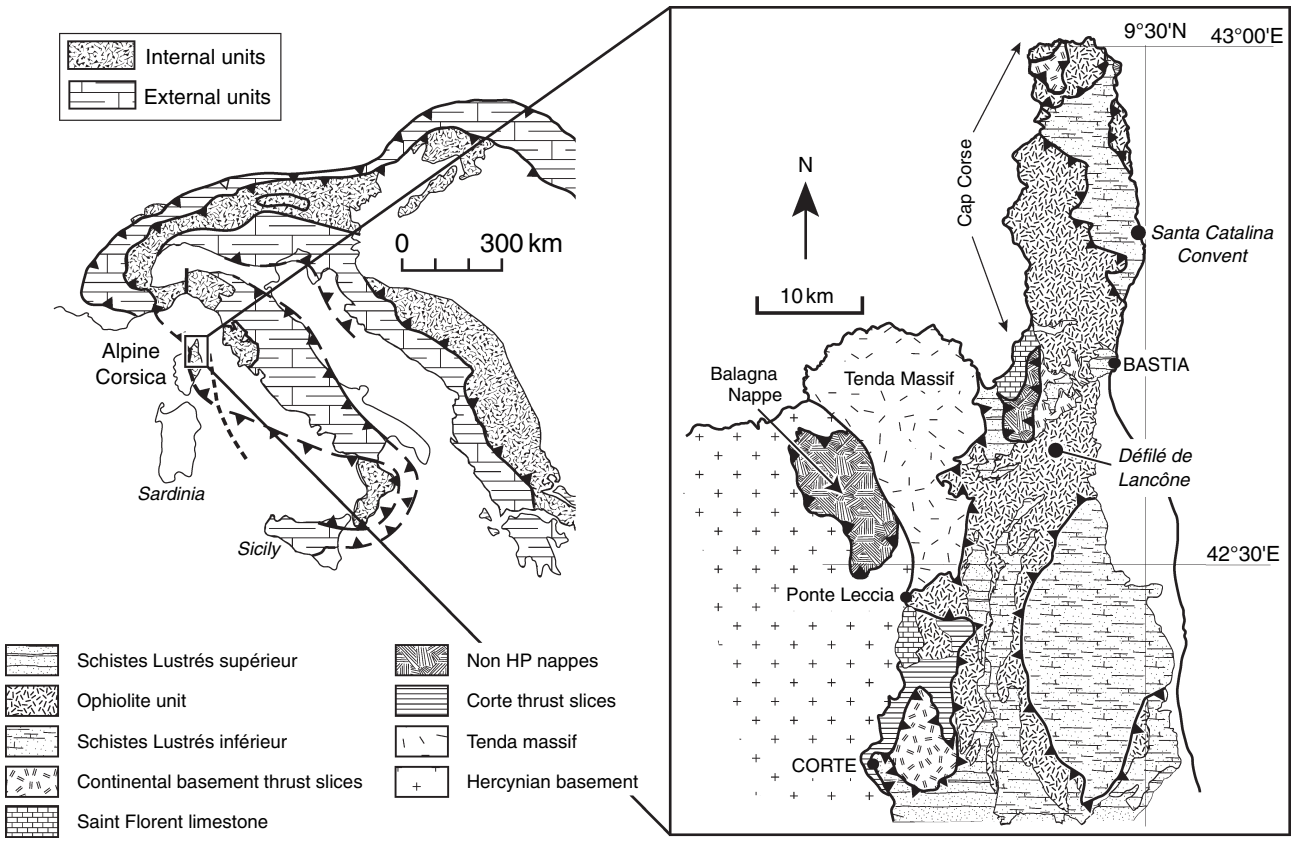

Fig. 1. Geological setting of the Corsican ophiolite complex showing its location within the European Alpine chain.

metamorphism are 1.5 GPa and 530 °C (Caron *et al.*, 1981; Fournier *et al.*, 1991; Lahondère, 1991). The eclogite facies mineral assemblages have been pervasively overprinted by a second high-pressure event in the blueschist facies with minimum P–T conditions of 0.9 GPa and 400 °C (Fournier *et al.*, 1991). The geothermal gradient at the time of both eclogite and blueschist facies metamorphism was fairly low < 15 °C km^{-1} which accounts for the presence of abundant lawsonite associated with both the eclogite and blueschist facies mineral assemblages. Exhumation and retrogression of the high-pressure nappes to greenschist facies occurred during the Eocene (Brunet *et al.*, 1997) when there was a switch from compressional to extensional tectonics (Daniel *et al.*, 1996; Malavielle *et al.*, 1998). Several studies have suggested that the transition from blueschist to greenschist facies was accompanied by a slight increase in temperature (Pequignot & Potdevin, 1984; Waters, 1989; Harris, 1984). However, Daniel *et al.* (1996) have suggested that temperatures during decompression were variable and decreased from 350–400 °C in the north-west to < 350 °C in the east. The greenschist facies retrogression has been dated at between 35 and 25 Ma (Maluski, 1977; Carpena *et al.*, 1979; Brunet *et al.*, 1997) and is associated with the formation of large, monomineralic albite veins within metabasalts of the ophiolite unit. The upper nappe stack, the Nappe Supérieur, appears to preserve only the effects of low-T sub-seafloor metamorphism (Warburton, 1986), and was thrust over previously exhumed and eroded high-pressure nappes during closure of the remnant Piedmont-Ligurian oceanic basin (Malavielle *et al.*, 1998).

SAMPLE COLLECTION AND ANALYTICAL TECHNIQUES

Albite veins from Alpine Corsica occur only in metabasalts and are limited geographically to Cap Corse and the region north-east of Corte (Fig. 1) where the effects of the greenschist facies overprint are most pronounced (e.g. Daniel *et al.*, 1996). Albite veins were collected from two locations: (1) the Défilé de Lancône, which is predominantly high-pressure ophiolitic material overlain by minor sedimentary rocks; and (2) in the vicinity of Santa Catalina Convent, where a high-pressure calcareous-metasedimentary rock is the dominant rock type with minor sheets of ophiolitic material (Fig. 1). A total of 10 albite veins was sampled from Alpine Corsica, seven from Défilé de Lancône and three from around the Santa Catalina Convent (Fig. 1). Hand samples were taken from: (1) the albite vein; (2) the albite vein alteration halo (altered wallrock); and (3) unaltered hostrock away from the albite vein. The exception to this was for two albite veins sampled from Défilé de Lancône, which were sampled on a centimetre scale using a hand brace with an 8 mm bit. The drill powder from the outer 2–3 mm of each sample was discarded. As the Corsican metabasalts are very fine-grained ($<<$ 1 mm), this procedure had no discernible effect on sample homogeneity. Hand samples were crushed in a Tema mill that was cleaned with ethanol and washed quartz between samples. Carbonate was removed with dilute HCl prior to silicate stable isotope analysis.

Oxygen isotope ratios of silicate samples were analysed at Monash University following the method of Clayton & Mayeda (1963) but using ClF_3 as the oxidizing reagent. Sample sizes were generally sufficient to yield > 100 μmol of CO_2 and isotopic ratios were measured on a Finnigan MAT 252 mass spectrometer. Values of $\delta^{18}O$ are reported in ‰ relative to SMOW (Standard Mean Ocean Water). NBS28 quartz analysed at the same time as the samples yielded $\delta^{18}O = 9.6 \pm 0.13$‰ ($n = 16$). The long-term average of NBS28 at Monash is 9.58 ± 0.12 (1σ). Oxygen and carbon isotope values of carbonates were analysed by extracting CO_2 from calcite by reaction of mixed carbonate–silicate powders with H_3PO_4 at 50 °C for 12–18 h, or calcite powders at 25 °C for 2–4 h, in sealed vessels, a modification of the technique of McCrea (1950). Appropriate acid correction factors were used in the processing of the data. The results are given relative to SMOW and PDB (Pee Dee Belemnite) respectively. Internal calcite standard ISACC-1 yielded $\delta^{13}C = -6.29 \pm 0.08$ and $\delta^{18}O = 12.62 \pm 0.15$‰ ($1\sigma$, $n = 12$). Reproducibility of silicate $\delta^{18}O$ analyses is ± 0.3‰, whilst reproducibility of carbonate $\delta^{18}O$ and $\delta^{13}C$ values is ± 0.15‰.

Whole-rock major element compositions were determined on fused lithium metaborate glass discs at the University of Melbourne using an ARL 4-20310 X-ray fluorescence spectrometer. Volatile loss on ignition was determined by weight loss at 1000 °C. SICAFE blank, BHVO-1 and G-2 rock standards were used to assess accuracy. Electron microprobe analyses of minerals were made using the electron microprobe facilities at the University of Melbourne (Cameca CAMEBAX SX50, 15 kV, 25 nA), the University of Adelaide (Cameca CAMEBAX SX51, 15 kV, 25 nA), and the University of Leeds, UK (Cameca CAMEBAX SX50, 15 kV, 12 nA, reduced to 10 nA when analysing lawsonite). Analyses were made using wavelength dispersive spectrometry, incorporating Cameca PAP matrix corrections. Total iron was analysed as FeO, and Fe_2O_3 contents for hydrous Fe-bearing silicates were recalculated using the methods outlined in Holland & Powell (1998) (see below). For all three universities, analyses were undertaken using a 1–2 μm beam size, with the exception of lawsonite (5 μm) and albite (3 μm). Values of 0.00 for weight per cent oxide totals indicate that the particular element was not detected. Mineral abbreviations are those defined by Kretz (1983).

PETROGRAPHY AND MINERAL CHEMISTRY

Two principal types of albite veins are recognized in the field. The first occurs as generally large dilatant

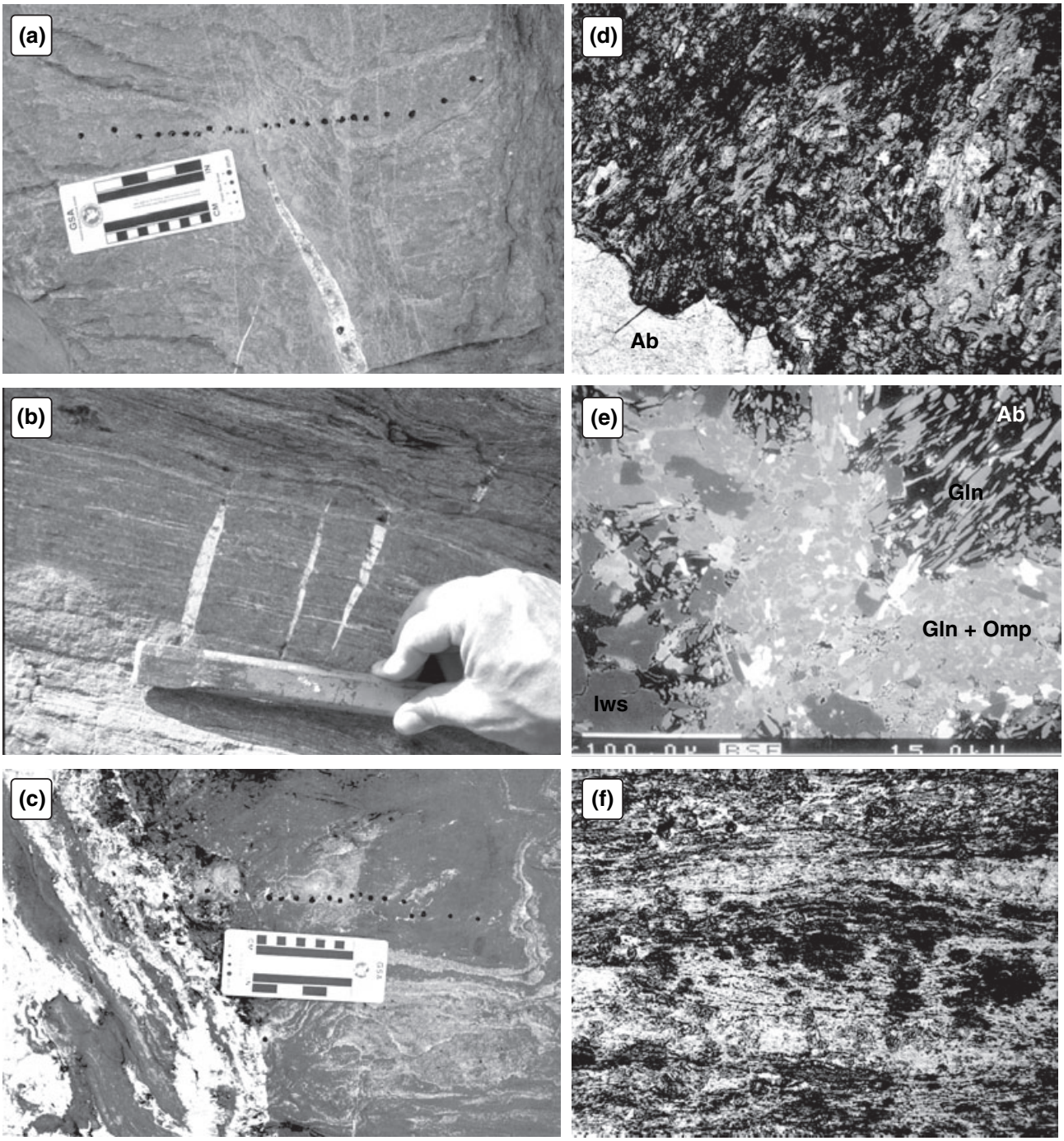

Fig. 2. (a) Termination of a large 15 cm wide albite vein from Défilé de Lancône. The pale zone around the terminal point of the vein is the greenschist facies alteration halo. The black dots indicate drilled sample sites for an oxygen isotope traverse across the vein. (b) Tension gashes in eclogitic metabasalts, now filled with albite. Chisel length is 15 cm. (c) Large albite vein with diffuse and irregular margin. Pale region to the right of the vein is not the vein alteration halo but the surface of a greenschist facies layer, exposed through spherical weathering of the host metabasalt. Black dots again indicate drilled sampling traverse. (d) Mineral assemblage on the margin of an albite vein, characterized by chlorite + actinolite + albite + clinozoisite. PPL, FOV = 0.3 cm. (e) Matrix mineral assemblage in host rocks to albite veins. BSE image, thin white bar at bottom left is 100 μm. (f) Foliation development in response to the greenschist facies overprint. PPL, FOV = 0.5 cm.

irregularly shaped fractures with locally very diffuse margins and anastomosing side stringers (Fig. 2a). These veins are on the order of 5–30 cm in width, are laterally continuous on a 2–3 m scale and are normally isolated features within a given outcrop. These veins usually crosscut the dominant foliation (retrograde) at

intermediate to high angles. The second occurs as smaller tension gashes normally less than 1 cm wide and less than 20 cm in length. The margins are normally sharper and the veins often occur in sets or groups of veins all showing a similar orientation normally high angle to the retrograde foliation (Fig. 2b). Both types of albite veins are generally monomineralic and are composed of coarse-grained (up to 1.5 cm diameter) granular albite grains that lack any preferred orientation. One of the albite veins had some calcite present, but in hand sample it occurs as clumps of large (0.5 mm) rhombohedral grains and is not considered to be synchronous with the main episode of albite vein formation (see Discussion below). In this study only the large albite veins were examined because of difficulties in sampling the smaller vein sets.

The albite veins have distinct alteration haloes up to 50 cm in width (the smaller veins having smaller alteration haloes) characterized by the development of pervasive greenschist facies mineralogies (Fig. 2c), formed by wall-rock infiltration of fluids apparently exsolved from the albite vein as it crystallized. The dominant minerals in the alteration haloes are actinolite, chlorite, epidote ($X_{Fe} > 0.5$) and albite (Fig. 2d), with minor calcite. Significantly, the alteration halo contains no quartz. Chlorite forms the dominant matrix mineral in the alteration haloes and occurs as large fibrous to granular mats with Mg# of *c*. 0.40. Some chlorite has appreciable amounts of Na, up to 0.3 cations pfu, probably indicating formation from the breakdown of sodic amphibole. Likewise actinolite, which occurs both as well-formed < 100 μm wide rhombohedral grains and as acicular needles within the chloritic matrix, has Na contents up to 0.33 cations pfu, indicating that actinolite is probably transitional in composition with glaucophane. There does not appear to be any systematic textural association of the rhombohedral *v*. acicular actinolite. The Mg# of actinolite can also be variable from 0.50 to 0.58 and depending on the amount of recalculated Fe^{3+} in the formula (Holland & Blundy, 1994) actinolite can have appreciable amounts of Al, up to 1.4 cations pfu. Epidote $[Fe^{3+}/(Fe^{3+} + Al^{3+} + Cr^{3+} - 2) \approx 0.62]$ occurs as porphyroblasts (up to 100 μm in diameter) also within the chloritic matrix, and is compositionally homogeneous but has inclusions of relict glaucophane. Porphyroblastic albite (Ab_{98}), up to 200 μm in diameter, contains numerous inclusions of acicular actinolite suggesting that its formation may have been late in the development of the alteration halo. Calcite, where present, occurs as equi-dimensional poorly shaped isolated grains randomly dispersed throughout the matrix. In addition, small blades of titanite occur disseminated throughout the matrix.

The alteration halo on the albite veins cross-cuts retrogressed blueschist and eclogite facies metabasaltic rocks. At the highest grades these metabasalts are composed of fine-grained interlocking mats of omphacite, in which well-developed laths of lawsonite and garnet porphyroblasts as well as minor titanite are dispersed. This assemblage was variably overprinted by blueschist facies mineralogies, where omphacite has been variably replaced by glaucophane, garnet became both more abundant and more Fe-rich, and albite porphyroblasts developed in the matrix. Lawsonite is still present but occurs as blocky rhombs rather than laths. These high-pressure assemblages have been affected by a variable greenschist facies overprint associated with the development of a semi-pervasive foliation defined by the development of chlorite and actinolite (Fig. 2e,f). Chlorite occurs as large mats of elongate chlorite grains on the order of 50–150 μm wide. The Mg#s of chlorite associated with the regional greenschist facies overprint are in general higher, up to 0.58 (although variable), than those of the greenschist alteration halo on the albite veins. Actinolite occurs as smaller (< 50 μm) well-formed rhombohedral grains with higher Mg#s but similar amounts of Na cations pfu than actinolite in the alteration halo indicating its transitional composition with glaucophane. Epidote and albite also developed during the regional greenschist facies overprint and occur as irregularly shaped, small (< 30 μm) grains dispersed throughout the chlorite + actinolite matrix. Epidote in the regional greenschist facies overprint has higher X_{Fe} values than the greenschist alteration halo up to 0.79, while albite is compositionally homogeneous and similar to the greenschist alteration halo is near end-member composition. Likewise, there is also no quartz present in either the retrograde or high-pressure mineral assemblages but titanite is present as patchy mats usually associated with chlorite, along with randomly distributed calcite grains. Representative compositions of minerals from the regional greenschist facies overprint and the greenschist facies alteration halo are shown in Table 1.

P–T ESTIMATES FOR ALBITE VEIN FORMATION

The *P–T* conditions of albite vein formation have been estimated using the vein alteration halo mineralogy (actinolite, chlorite, epidote and albite), which is considered to have formed synchronously with the albite vein (from petrographic observations), and mineral compositions are given in Table 1(a). End-member activities of these minerals were calculated using the program AX (Holland & Powell, 1998) and a set of independent reactions were calculated between these end-members using the thermodynamic program THERMOCALC (Holland & Powell, 1998). The reactions generated were all dehydration reactions with the average intersection of the reactions found at 478 ± 31 °C (1σ) and 0.37 ± 0.14 GPa (1σ), assuming an activity of H_2O equal to 1.0. This is probably a realistic assumption as lawsonite is metastable for any appreciable value of X_{CO_2}. In any event, the effect of decreasing X_{H_2O} from 1.0 to 0.8 caused no appreciable difference in the *P–T* estimates, whilst dropping

Table 1a. Representative mineral compositions from the greenschist facies alteration halo around albite veins.

Wt %	Ab	Ab	Ep	Ep	Chl	Chl	Chl	Act	Act	Act
Wt% oxide										
SiO_2	67.84	69.26	37.40	38.06	27.51	26.81	26.10	52.40	53.00	50.20
TiO_2	0.01	0.06	0.34	0.11	0.03	0.02	0.07	0.04	0.06	0.00
Al_2O_3	18.73	19.15	24.00	24.55	18.65	18.54	18.80	3.06	2.09	3.14
Cr_2O_3	0.06	0.00	0.00	0.04	0.01	0.12	0.00	0.03	0.00	0.00
FeO	0.18	0.11	9.38	9.67	24.52	23.98	19.19	13.57	12.90	11.13
MnO	0.00	0.03	0.52	0.28	0.36	0.33	0.31	0.22	0.22	0.26
MgO	0.01	0.00	0.00	0.02	16.14	15.94	16.20	13.64	14.70	15.10
CaO	0.10	0.20	22.80	22.88	0.04	0.07	0.18	11.03	11.50	10.50
Na_2O	11.09	10.87	0.00	0.00	0.01	0.00	1.17	1.15	1.56	0.85
K_2O	0.02	0.03	0.07	0.00	0.04	0.02	0.00	0.11	0.12	0.05
Total	98.04	99.71	94.51	95.61	87.31	85.83	82.02	95.25	96.15	91.23
Cation totals										
Oxygen	8	8	12.5	12.5	14	14	14	23	23	23
Si	3.02	3.02	3.05	3.04	2.90	2.87	2.74	7.65	7.03	7.48
Ti	0.00	0.00	0.02	0.01	0.00	0.00	0.01	0.00	0.01	0.00
Al	0.98	0.99	2.31	2.31	2.31	2.34	2.33	0.53	1.45	0.55
Cr	0.00	0.00	0.00	0.00	0.00	0.01	0.00	0.00	0.00	0.00
Fe^{3+}	0.01	0.00	0.44	0.61	0.00	0.00	0.41	0.24	1.56	0.42
Fe^{2+}	0.00	0.00	0.20	0.04	2.16	2.15	1.69	1.66	0.00	1.39
Mn	0.00	0.00	0.04	0.02	0.03	0.03	0.03	0.03	0.04	0.03
Mg	0.00	0.00	0.00	0.00	2.53	2.54	2.54	2.97	2.19	3.35
Ca	0.01	0.01	1.99	1.96	0.01	0.01	0.02	1.72	2.10	1.68
Na	0.96	0.92	0.00	0.00	0.00	0.00	0.24	0.33	0.21	0.25
K	0.00	0.00	0.01	0.00	0.01	0.00	0.00	0.02	0.01	0.01
Total	4.98	4.94	8.06	7.99	9.95	9.954	10.01	15.15	14.60	15.16
			X_{Ep} 0.59	0.66	Mg# 0.40	0.40	0.46	0.50	0.53	0.58

Table 1b. Representative mineral compositions from the regional greenschist facies overprint.

Wt%	Ab	Ab	Ep	Ep	Chl	Chl	Chl	Act	Act	Act
Wt% oxide										
SiO_2	68.36	68.91	37.82	37.59	27.26	30.62	26.50	54.72	55.68	55.94
TiO_2	0.00	0.00	0.02	0.04	0.00	0.06	0.00	0.00	0.03	0.00
Al_2O_3	19.31	19.22	25.44	23.48	19.35	16.69	19.39	2.65	0.60	0.49
Cr_2O_3	0.00	0.00	0.05	0.16	0.07	0.15	0.11	0.04	0.00	0.07
FeO	0.33	0.20	9.48	11.73	23.40	22.18	24.36	11.43	10.94	10.81
MnO	0.00	0.02	0.06	0.00	0.28	0.35	0.27	0.29	0.25	0.15
MgO	0.01	0.00	0.00	0.01	16.99	16.17	15.93	15.82	16.56	16.94
CaO	0.28	0.08	23.73	23.88	0.12	1.43	0.08	10.83	12.20	12.56
Na_2O	11.91	12.33	0.04	0.05	0.07	0.27	0.04	1.31	0.64	0.42
K_2O	0.04	0.00	0.00	0.02	0.00	0.37	0.00	0.51	0.05	0.05
Total	100.24	100.76	96.64	96.96	87.54	88.29	86.68	97.60	96.95	97.43
Cation totals										
Oxygen	8	8	12.5	12.5	14	14	14	23	23	23
Si	2.99	2.99	2.99	2.99	2.85	3.15	2.81	7.81	7.99	7.98
Ti	0.00	0.00	0.00	0.00	0.00	0.01	0.00	0.00	0.00	0.00
Al	0.99	0.99	2.37	2.20	2.38	2.03	2.43	0.45	0.10	0.08
Cr	0.00	0.00	0.00	0.01	0.01	0.01	0.01	0.01	0.00	0.01
Fe^{3+}	0.01	0.01	0.63	0.78	0.00	0.00	0.00	0.10	0.00	0.00
Fe^{2+}	0.00	0.00	0.00	0.00	2.04	1.91	2.16	1.27	1.31	1.29
Mn	0.00	0.00	0.00	0.00	0.03	0.03	0.02	0.04	0.03	0.02
Mg	0.00	0.00	0.00	0.00	2.64	2.48	2.52	3.37	3.54	3.60
Ca	0.01	0.00	2.01	2.03	0.01	0.16	0.01	1.66	1.88	1.92
Na	1.01	1.04	0.01	0.01	0.01	0.05	0.01	0.36	0.18	0.12
K	0.00	0.00	0.00	0.00	0.00	0.05	0.00	0.09	0.01	0.01
Total	5.01	5.03	8.01	8.02	9.97	9.88	9.97	15.16	15.04	15.03
			X_{Ep} 0.63	0.79	Mg# 0.42	0.58	0.40	0.58	0.60	0.61

Fe^{3+} in amphibole from Holland & Blundy (1994); Fe^{3+} in epidote and chlorite recalculated based on cation totals; Fe in albite assumed to be Fe^{3+}; $X_{Ep} = Fe^{3+}/(Fe^{3+} + Al + Cr^{3+} - 2)$ after Franz & Liebscher (2004); Mg# = MgO/(MgO + FeO).

X_{H_2O} to 0.5 resulted in the temperature and pressure estimates dropping by *c.* 20 °C and 0.06 GPa respectively.

Using the same method, *P–T* conditions for the regional greenschist facies overprint were estimated using minerals considered to have developed during this event. Chlorite, actinolite, epidote and albite mineral compositions are given in Table 1(b). The slight compositional differences in these minerals, particularly actinolite and chlorite, between the alteration halo and the regional greenschist event resulted in a different set of independent reactions being gen-

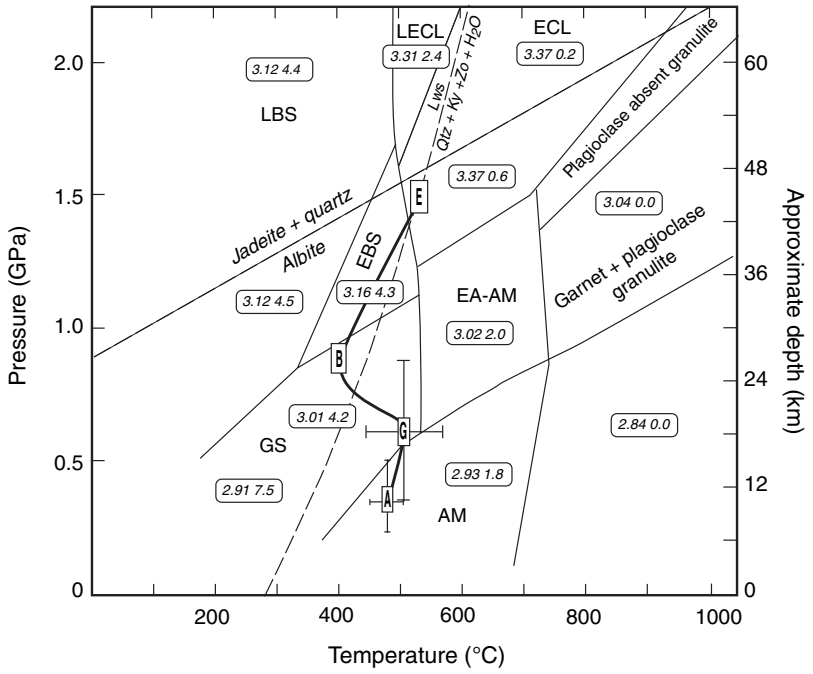

Fig. 3. Alpine Corsica *P–T* conditions for the eclogite and blueschist facies metamorphism from the literature and for the greenschist facies retrogression and albite vein formation calculated in this study. Boxes with error bars are from this study. Ecologite and blueschist *P–T* conditions for Alpine Corsica from Caron (1994) and Malavielle *et al.* (1998). Metamorphic facies after Bousquet *et al.* (1997). Numbers in rectangles are density (3-digit) and water content (2-digit) also after Bousquet *et al.* (1997). Positions of the terminal reactions for albite and lawsonite stability (indicated by dashed lines) calculated using the Holland & Powell (1998) data set. Abbreviations for *P–T* path as follows: E, ecologite; B, blueschist; G, greenschist; A, albite vein. Abbreviations for facies as follows: AM, amphibolite; EBS, epidote blueschist; LBS, lawsonite blueschist; GS, greenschist; LECL, lawsonite eclogite; ECL, eclogite; EA-AM, epidote–albite amphibolite.

erated not all of which were dehydration reactions. The calculated intersection was found at 507 ± 31 °C (1σ) and 0.62 ± 0.13 GPa (1σ) assuming the activity of H_2O is 1.0. However, dropping X_{H_2O} to 0.8 and then 0.5 caused little difference in the estimated temperature (< 10 °C), while the estimated pressure decreased by ~0.12 GPa. Comparison of these results indicates that while there is little difference in the temperature estimates given the error estimates, there is a notable difference in the pressure estimates with the albite veins appearing to have formed in response to decompression occurring directly after the regional greenschist facies event (Fig. 3). This interpretation is consistent with petrographic observations that the alteration halo on the albite veins cross-cuts and thus postdates the regional greenschist facies fabric.

STABLE ISOTOPE GEOCHEMISTRY

General oxygen isotope systematics

Table 2 and Fig. 4 summarize the stable isotope data for the albite veins from Alpine Corsica. The $\delta^{18}O_{ab}$ values of the albite veins vary between 11.0 and 15.9‰ with the $\delta^{18}O$ values of veins from Santa Catalina Convent being slightly higher and more variable than those from Défilé de Lancône. One vein from Défilé de Lancône contained calcite with a $\delta^{18}O_{cc}$ value of 16.7‰ and a $\delta^{13}C_{cc}$ value of −0.5‰. At Défilé de Lancône and Santa Catalina Convent, the $\delta^{18}O_{wr}$ values of the alteration halo vary between 6.0 and 13.4‰ and between 8.2 and 12.9‰ respectively. At Défilé de Lancône, $\delta^{18}O_{wr}$ values of the unaltered hostrocks show a much narrower range of values than the alteration halo, varying between 6.6 and 9.1‰. In contrast, at Santa Catalina Convent, $\delta^{18}O_{wr}$ values of the unaltered hostrocks are higher than those of the alteration halo, varying between 10.7 and 13.8‰.

Oxygen isotope traverses JM96CO73-94 and JM96CO154-174

Figure 5 shows oxygen isotope profiles for two albite vein traverses sampled using small-scale drilling. Data for these traverses are presented in Table 3. Both the veins are from Défilé de Lancône (Fig. 1c), where the highest metamorphic grade reached was lawsonite eclogite. In both the traverses the $\delta^{18}O_{ab}$ value of the albite vein (11.7–12.5‰) is between 3.3 and 4.2‰ higher than the $\delta^{18}O_{wr}$ of the surrounding alteration halo (Table 3). For traverse JM96CO73-94, the alteration halo has an average $\delta^{18}O_{wr}$ value of 9.2 ± 0.4‰, while traverse JM96CO154-174 has a slightly lower average $\delta^{18}O_{wr}$ value of 8.3 ± 0.5‰. For both traverses, the unaltered hostrock has an average $\delta^{18}O_{wr}$ value of 9.4 ± 0.5‰.

Stable isotope geochemistry of calcite

Calcite is present as a minor phase in both the altered wallrocks and the unaltered hostrocks but is more commonly present in the altered wallrock (greenschist alteration halo). For Défilé de Lancône, only one sample of partially retrogressed hostrock contained calcite with a $\delta^{18}O_{cc}$ value of 12.7‰ and a $\delta^{13}C_{cc}$ value of 2.1‰. In contrast, four samples of altered wallrock contained calcite with $\delta^{18}O_{cc}$ values between 12.9 and 16.9‰ and $\delta^{13}C_{cc}$ values between −0.5 and 1.8‰. Only

Table 2. Stable isotope geochemistry of Corsican albite veins.

Sample no.	Albite veins (‰)			Whole rocks (‰)			Description
	$\delta^{18}O_{wr}$	$\delta^{18}O_{cc}$	$\delta^{13}C_{cc}$	$\delta^{18}O_{wr}$	$\delta^{18}O_{cc}$	$\delta^{13}C_{cc}$	
Défilé de Lancône Vein #1							
JM96CO175	12.2						Ab-vein
JM95CO119				6.0			Retrogressed LBS-LECL
JM95CO131				10.0			Retrogressed LBS-LECL
JM95CO117				7.4	15.7	−0.5	Laws BS-ECL
Défilé de Lancône Vein #2							
JM95CO152	14.3	16.7	−0.5	13.4	16.9	−0.4	Ab-vein with GS alteration halo
JM95CO134				8.5			Retrogressed LBS-LECL
JM95CO140a				9.7	16.7	0.3	Retrogressed LBS-LECL
JM95CO142				9.7			LBS-LECL
JM95CO143				9.1			LBS-LECL
Défilé de Lancône Vein #3							
JM95CO153A	11.2			8.6			Ab-vein with GS alteration halo
JM95CO153B				9.4			GS wallrock to Ab-vein JM95CO153a
JM95CO145				6.6			LBS-LECL
Défilé de Lancône Vein #4							
JM95CO183	11.7						Ab-vein
JM95CO184				8.7			GS wallrock to JM95CO183 Ab-vein
JM95CO164				6.6			Retrogressed LBS-LECL
JM95CO165				6.9			LBS-LECL
Défilé de Lancône Vein #5							
JM97CO43	11.0						Ab-vein
JM97CO44				6.8	12.9	1.8	GS wallrock to JM97CO43 Ab-vein
JM97CO45				8.2	12.7	2.1	Retrogressed LBS-LECL near JM97CO43
Santa Catalina Convent Vein #1							
JM96CO69	15.9						Ab-vein
JM96CO68				12.9	19.1	1.4	GS wallrock to Ab-vein JM96CO69
JM96CO70				11.5	18.2	1.0	GS wallrock to Ab-vein JM96CO69
JM96CO71				11.7	18.1	0.9	GS wallrock to Ab-vein JM96CO69
JM96CO72				11.6	20.1	−0.4	Retrogressed LBS
Santa Catalina Convent Vein #2							
JM96CO273	13.6						Ab-vein near JM96CO69
JM96CO269				10.7			GS wallrock to Ab-vein JM96CO273
JM96CO268				13.8			LBS-LECL
JM96CO267				12.0			LBS-LECL
Santa Catalina Convent Vein #3							
JM96CO362	11.5						Ab vein
JM96CO361				8.2			GS alteration halo to Ab-vein JM96CO362

GS, greenschist; LBS, lawsonite blueschist; LECL, lawsonite eclogite.

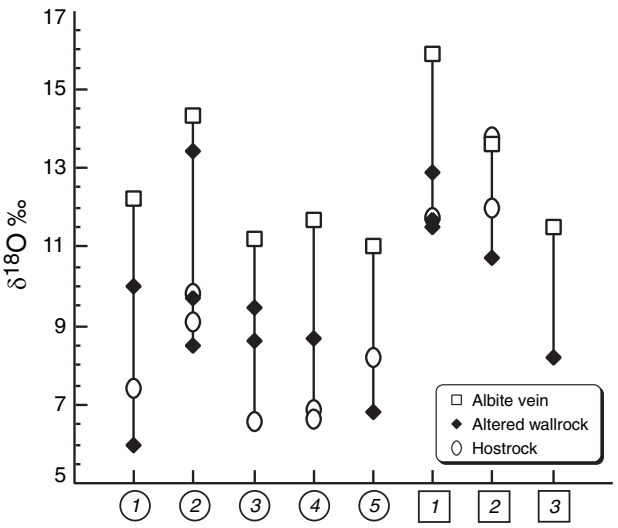

Fig. 4. Oxygen isotope variation between the alteration halo and unaltered hostrocks associated with albite veins from Alpine Corsica. Data from Table 2. Numbers in circles are albite veins from Défilé de Lancône. Numbers in squares are albite veins from Santa Catalina.

one albite vein contained calcite, with a $\delta^{18}O_{cc}$ value of 16.7‰ and a $\delta^{13}C_{cc}$ value of −0.5‰ (Table 2). This calcite appears to be in equilibrium with calcite in the altered wallrocks, that has almost identical values. There is no systematic variation in $\delta^{18}O_{cc}$ with $\delta^{18}O_{wr}$ values. Similar patterns are observed for samples from Santa Catalina Convent, where the altered wallrock contains calcite with $\delta^{18}O_{cc}$ values of between 18.1 and 20.1‰ and $\delta^{13}C_{cc}$ values of between −0.4 and 1.4‰. Again there appears to be no systematic variation in $\delta^{18}O_{cc}$ with $\delta^{18}O_{wr}$ values.

MAJOR ELEMENT GEOCHEMISTRY

The major element geochemistry is given in Table 4 and shown in Fig. 6 as a ratio between the wt% oxide in the alteration halo (altered wallrock) and wt% oxide in the unaltered hostrocks from five of the albite veins. No change in wt% oxide between the alteration halo and unaltered hostrocks would be equal to a value of 1. This analysis of the data does not take into account volume or mass changes that would be associated with the development of more hydrous mineral assemblages

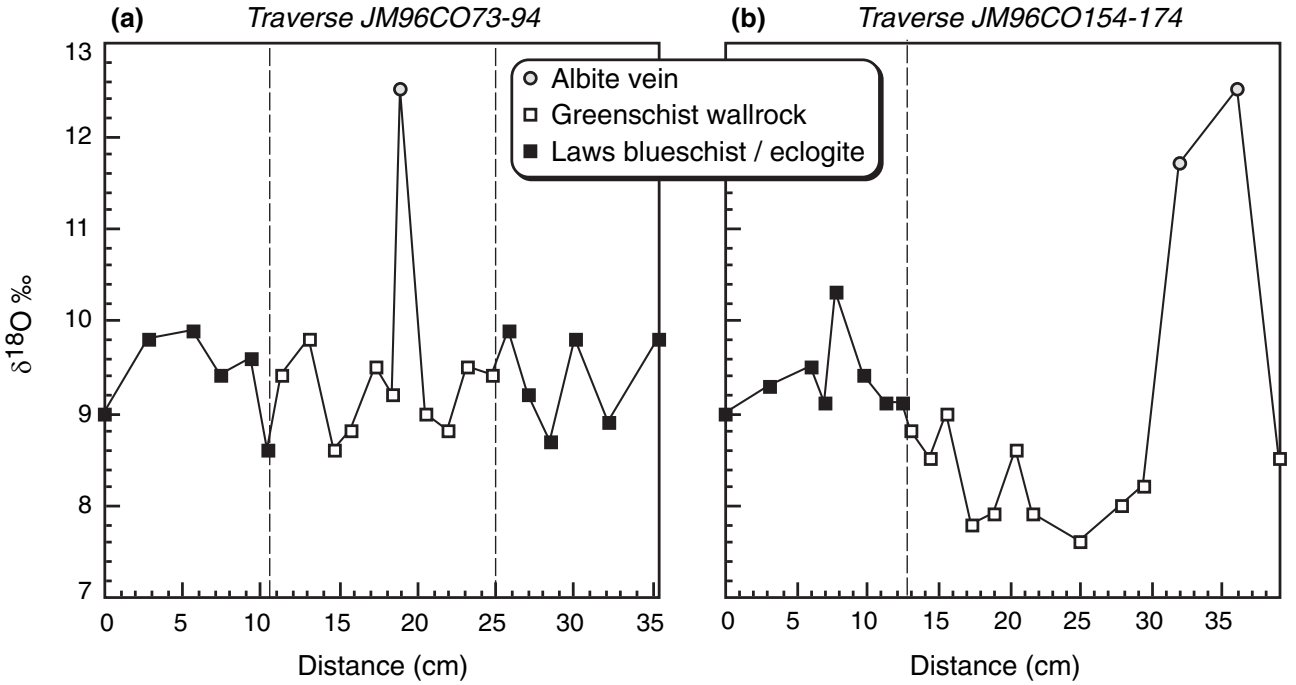

Fig. 5. Oxygen isotope traverses across two albite veins from Défilé de Lancône, Alpine Corsica.

in the alteration halo of the albite veins. However, a Gresen's style analysis of the data which takes into account volume and/or mass changes is not feasible, as this relies on the identification of immobile elements, normally taken as Al or Ti, which in the case of the albite veins, is clearly not realistic. Unaltered hostrocks that were clearly outside the mineralogical alteration halo on the albite veins were sampled between 1 and 3 m from the veins. In general, there is no systematic depletion or addition of any one component within the alteration halo. For the three vein components, Na, Si and Al, only Na shows any significant variation, with three of the albite veins showing gains of up to 154% Na_2O in the alteration halo and two of the veins showing losses of 10% Na_2O. For Al_2O_3, all five veins showed losses in the alteration halo of between 6 and 4%, while four veins showed SiO_2 gains of up to 12%, with one vein recording a loss of only 1%. None of the albite veins recorded losses of all three vein components within the alteration halo.

Closer analysis of the data set indicates that variations in the patterns of addition or depletion within the vein alteration halo are related in part to original composition variations in the hostrocks. Figure 6(b) compares the mean compositions of unaltered hostrock and altered wallrock with 95% confidence error bars indicated. Although the small number of samples makes it difficult to do any realistic statistical comparison, significant overlaps do occur for most of the major oxides, suggesting that taken as a whole the two groups of data are not statistically distinct. However, there are two points to note: (1) comparison of the mean wt% Al_2O_3 for the altered wallrocks and unaltered hostrocks suggests that the two are extremely close to representing distinct ranges with the alteration halo having a higher Al_2O_3 composition; and (2) the altered wallrocks have more varied compositions than the hostrocks, which probably reflects heterogeneous fluid–rock interaction on a scale of tens of cm. The high Al_2O_3 contents of the alteration halo are unusual in that if the vein material has been derived from the immediate wallrock, a depletion in Al_2O_3 would be expected. Conversely the mean wt% SiO_2 and Na_2O for the altered halo are slightly lower than that of the hostrock although at the 95% level the values are not statistically different.

DISCUSSION

Relationship between calcite and albite veins

The $\delta^{13}C_{cc}$ values of around 0‰ for the one calcite-bearing albite vein and calcite in the altered wallrocks and hostrocks indicate that the calcite is sedimentary in origin (Hoefs, 1997; Fig. 7). The two possible sources for the calcite are therefore: (1) direct precipitation from circulating seawater during hydrothermal subseafloor alteration prior to subduction and high-pressure metamorphism; or (2) from CO_2-bearing fluids derived from the overlying calcareous metasediments (the Schistes Lustrés). Distinguishing between these two options should be possible by looking at the relationship between the $\delta^{18}O$ value of the calcite and that of the host metabasic rocks. Ganor *et al.* (1994)

Table 3. $\delta^{18}O$ values for the two drilled Corsican albite vein traverses.

Sample no.	Rock type	Dist (cm)	$\delta^{18}O_{wr}$ (‰)
Défilé de Lancône Albite vein traverse 1			
JM96CO73	BS	0.0	9.0
JM96CO74	BS	2.8	9.8
JM96CO75	BS	5.7	9.9
JM96CO76	BS	7.5	9.4
JM96CO77	BS	9.3	9.6
JM96CO78	BS	10.5	8.6
BS/GS contact		10.6	
JM96CO79	GS	11.3	9.4
JM96CO80	GS	13.1	9.8
JM96CO81	GS	14.7	8.6
JM96CO82	GS	15.8	8.8
JM96CO83	GS	17.3	9.5
JM96CO84	GS	18.4	9.2
JM96CO95	Alb vein	19.0	12.5
JM96CO85	GS	20.5	9.0
JM96CO86	GS	21.9	8.8
JM96CO87	GS	23.2	9.5
JM96CO88	GS	24.8	9.4
BS/GS contact		25.0	
JM96CO89	BS	25.9	9.9
JM96CO90	BS	27.1	9.2
JM96CO91	BS	28.5	8.7
JM96CO92	BS	30.1	9.8
JM96CO93	BS	32.2	8.9
JM96CO94	BS	35.4	9.8
Défilé de Lancône Albite vein traverse 2			
JM96CO154	BS	0.0	9.0
JM96CO155	BS	3.2	9.3
JM96CO156	BS	6.0	9.5
JM96CO157	BS	7.1	9.1
JM96CO158	BS	7.8	10.3
JM96CO159	BS	9.7	9.4
JM96CO160	BS	11.4	9.1
JM96CO161	BS	12.4	9.1
BS/GS contact		12.8	
JM96CO162	GS	13.1	8.8
JM96CO163	GS	14.4	8.5
JM96CO164	GS	15.6	9.0
JM96CO165	GS	17.4	7.8
JM96CO166	GS	19.0	7.9
JM96CO167	GS	20.5	8.6
JM96CO168	GS	21.6	7.9
JM96CO169	GS	25.0	7.6
JM96CO170	GS	27.8	8.0
JM96CO171	GS	29.4	8.2
JM96CO172	Alb vein	32.0	11.7
JM96CO173	Alb vein	36.0	12.5
JM96CO174	GS	39.0	8.5

Dist, distance; BS, blueschist; GS, greenschist.

determined that the fractionation between calcite and the silicate fraction of a rock could be calculated as $\Delta^{18}O_{(calcite\text{-}whole\ rock)} = (6.4\text{–}6.8I) \times 10^6 \times T^{-2}$, where I (the Garlick Index; Garlick, 1966) is a measure of the chemical composition of the rock and T is temperature in Kelvin. The expected range of $\Delta^{18}O_{cc\text{-}wr}$ fractionations, assuming a range of I-values relevant to high-pressure metabasalts (0.68–0.73: Ganor *et al.*, 1994; Miller *et al.*, 2001) and a vein temperature of 470 °C, should be *c.* 1.6–2.2‰. In the course of this study only five samples containing calcite were analysed for both $\delta^{18}O$ values and whole-rock geochemistry. Of these five samples, two were retrogressed samples from within the albite vein alteration halo ($\Delta^{18}O_{cc\text{-}wr} = 6.3‰$), one was from the regional greenschist facies overprint ($\Delta^{18}O_{cc\text{-}wr} = 7.0‰$) and two were from unretrogressed lawsonite–blueschist metabasalts ($\Delta^{18}O_{cc\text{-}wr} = 8.4‰$). Although this is a somewhat limited database, these fractionations are considerably larger than the predicted values and suggest that the calcite formed at lower temperatures than the albite veins, thus post-dating the veins. This is consistent with the stable isotope data from the one albite vein, where the difference between the $\delta^{18}O$ values of calcite and albite in the vein is equal to 2.4‰, which equates to a temperature of 210 °C, using the fractionation data of Clayton *et al.* (1989). This temperature cannot be representative of the temperature of albite vein formation as at this temperature pumpellyite, prehnite and Na–Ca–zeolites rather than Ca-amphibole would form in the alteration halo. Thus the calcite seems to be a manifestation of late fluid flow possibly derived from decompression of the Schistes Lustrés nappe (Cartwright & Buick, 2000).

Chemical transport distances

The elements required for albite vein formation (Si, Na and Al) may have been derived from the immediate vicinity of the albite vein or they may have been derived from a larger area. If one or more of Si, Al and Na were derived from the immediate vicinity of the

Table 4. Major element geochemistry for altered wallrock/unaltered hostrock pairs adjacent to albite veins from Alpine Corsica.

	96–68	96–72	95–119	95–117	95–134	95–142	95–153a	95–145	95–184	95–165
XRF wt% oxide										
SiO_2	43.03	46.65	46.81	51.14	48.77	49.35	45.54	50.80	49.53	49.14
TiO_2	1.45	1.85	1.16	1.09	1.67	2.03	2.30	1.28	1.21	1.43
Al_2O_3	16.28	15.26	15.91	14.36	17.02	14.69	14.42	13.28	16.97	15.41
Fe_2O_3	9.15	11.72	10.91	8.00	9.84	11.57	13.12	12.04	8.53	8.62
MgO	3.65	4.86	9.40	8.43	7.38	5.62	7.60	6.09	9.45	6.65
MnO	0.18	0.34	0.32	0.37	0.14	0.24	0.20	0.19	0.19	0.32
CaO	13.64	11.58	7.13	7.70	5.64	7.84	11.71	7.89	4.23	9.64
Na_2O	1.39	3.53	3.55	4.66	4.83	4.35	2.12	4.56	5.04	4.52
K_2O	3.12	0.67	0.01	0.01	0.02	0.11	0.01	0.55	0.07	0.04
SO_3	b.d.	b.d.	0.01	b.d.	0.16	b.d.	b.d.	b.d.	0.10	0.07
P_2O_5	0.18	0.31	0.14	0.14	0.06	0.20	0.18	0.18	0.10	0.07
LOI	7.29	2.91	4.12	3.95	4.18	3.54	2.56	2.80	4.42	3.27
Total	99.36 WA	99.68 HO	99.92 WA	99.85 HO	99.71 WA	99.54 HO	99.76 WA	99.66 HO	99.84 WA	99.18 HO

WA, alteration halo; HO, unaltered hostrock; b.d., below detection limits; LOI, loss on ignition.

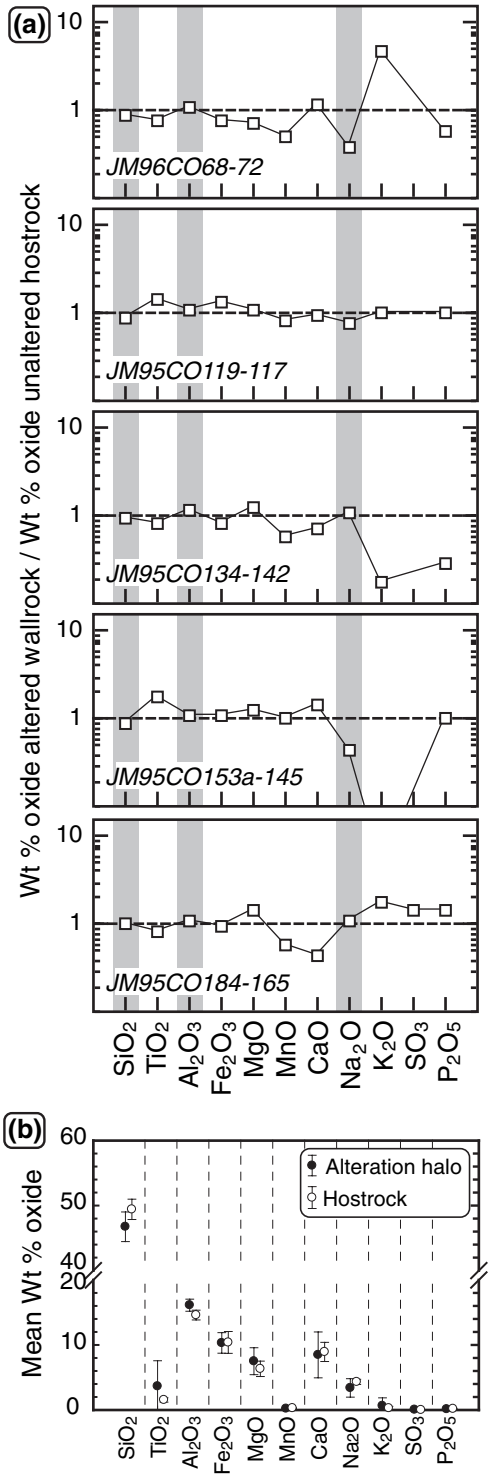

Fig. 6. (a) Whole-rock geochemistry from the Corsican albite veins plotted as a ratio of the wt% of each oxide in the altered wallrock over the unaltered hostrock. Values greater than 1 indicate addition of components to the altered wallrock, whereas values less than 1 indicate depletions. Grey bands highlight the three vein forming components, Na, Si and Al. (b) Comparison between the mean wt% value for individual oxides for the albite vein alteration haloes and the hostrocks. Error bars are 95% confidence. Data from Table 5.

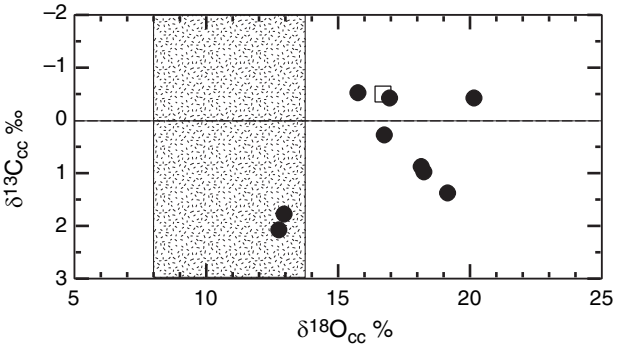

Fig. 7. $\delta^{13}C$ *v.* $\delta^{18}O$ plot for calcite in the veins, and associated wallrocks. Whilst $\delta^{18}O_{cc}$ values are variable, $\delta^{13}C_{cc}$ values are close to 0% and are indicative of a sedimentary origin for the calcite. Filled circles represent whole-rock analyses while the one open square is the single albite vein that contained calcite. Shaded region indicates range of silicate $\delta^{18}O$ values for the ophiolitic rocks (data from Miller *et al.*, 2001).

albite vein, there should be significant and consistent depletions in these elements within the alteration halo. Such a system has been documented from Zermatt-Saas in Switzerland, where prominent depletion zones of SiO_2 and Al_2O_3 next to quartz–kyanite veins attests to a local, probably diffusive transport, origin of the veins (Widmer & Thompson, 2001). Such a result is consistent with the observation that at the high pressures at which quartz–kyanite veins form (> 1 GPa), fluid flow becomes restricted to grain-scale processes (Philippot & Selverstone, 1991; Selverstone *et al.*, 1992), thus limiting the distance over which chemical transport via a fluid phase is likely to occur. However, albite veins are far more ubiquitous and volumetrically significant than quartz–kyanite veins and their formation is normally taken to imply advective mass transport via fractures or fracture networks. Again this is consistent with observations in other high-pressure terranes that retrograde fluid flow at pressures < 1 GPa (i.e. the conditions under which the albite veins would form) is fracture hosted (Fisher & Byrne, 1990; Barrientos, 1991; Barrientos & Selverstone, 1993; Bebout & Barton, 1993).

As pointed out above for the Corsican albite veins, Al_2O_3 seems to have elevated compositions in the alteration halo when compared with the hostrocks whilst SiO_2 and Na_2O seem to be depleted overall in the alteration halos. As the albite veins require a net transfer of aluminium to the site of albite vein formation, it is difficult to reconcile the increased Al_2O_3 contents of the alteration halo which imply advection of material outwards from the fracture. This type of pattern has been highlighted by Oliver & Bons (2001) as indicative of open-system veining where they suggest that changes in pressure upon fracture formation can lead to complex interplays between mineral solubilities, diffusion, dispersion and advection processes in three dimensions that result in quite different mass transfer

patterns than those that would be generated by simple infiltration. Such a situation is highly relevant for albite veining as aluminium, which is normally taken to be largely immobile, must clearly have been brought to the site of vein precipitation in significant quantities. Thus, the mass imbalances between the changes in the altered wallrock compositions relative to the unaltered hostrocks and the amount of albite in the veins, clearly implies transport over a distance greater than the immediate wallrock zone.

Source of the vein-forming fluid

The likely $\delta^{18}O$ value of the vein-forming fluid can be calculated using the temperature of vein formation and the Ab–H_2O fractionation data of Friedman & O'Neil (1977). At 470 °C, the fractionation between albite and H_2O is 1.6‰, indicating that the $\delta^{18}O$ value of the vein-forming fluid for the Corsican albite veins was between 9.4 and 14.3‰. Figure 8 shows the $\delta^{18}O$ ranges for all the major rock types from Alpine Corsica (data from Miller *et al.*, 2001). The $\delta^{18}O$ values for the vein-forming fluid calculated above correlate most closely with the metabasaltic units of the ophiolite. The absence of albite veins in the serpentinites and gabbros, combined with their lower $\delta^{18}O$ values indicates that they are unlikely to be the source of the fluids. The other rock types, including sedimentary rocks of the Schistes Lustrés, have $\delta^{18}O$ values that are in general too high for the fluids to have been sourced directly from these rocks (Fig. 8). In addition, the chemistry of such fluids would make them unlikely sources for the formation of albite veins. The formation of albite in the veins requires a high Na to K ratio in the vein-forming fluid, as discussed below. A fluid derived from the Schistes Lustrés or the granites on Corsica would be unlikely to have such a chemistry as these white mica-rich rock types have relatively high K_2O coupled with a low Na_2O contents. In comparison, the metabasalts contain up to 5 wt% Na_2O but negligible K_2O (Table 4). Cartwright & Buick (2000) suggested that fluid flow on Corsica leading to the generation of extensive quartz–calcite veining in the Schistes Lustrés was probably on the scale of metres to hectometres with little input from the ophiolitic units. The general lack of quartz–calcite veins in the ophiolitic units and albite veins in the Schistes Lustrés units supports the lack of large-scale fluid exchange between the two rock packages. Thus it seems the albite veins are derived from locally generated fluid flow within the metabasaltic units.

Chemical controls on vein formation

There are a number of chemical factors that may control or influence the formation of albite veins during exhumation of high-pressure terranes, including pressure, temperature, pH, X_{CO_2}, salinity, the solubilities of Na, Si and Al, the ratio of Na to K in the fluid, and Al-complex formation. Some of the most important questions regarding the chemical control on albite vein formation are: (1) what is the chemical composition of the vein forming fluid; (2) why is albite precipitated and not other silicate minerals; and (3) what causes the precipitation of albite from a fluid. In this study, we have identified four chemical factors that are important in understanding albite vein formation. These are: (1) the degree of silica saturation in the fluid; (2) the Na:K ratio in the fluid; (3) the solubility of Al; and (4) the influence of Al-speciation. To investigate these questions a series of $\log(a\mathrm{Na}^+/a\mathrm{H}^+)$ *v.* $\log(a\mathrm{K}^+/a\mathrm{H}^+)$ (Fig. 9) and $\log(a\mathrm{Na}^+/a\mathrm{H}^+)$ *v.* $\log(a\mathrm{Al}^{3+}/(a\mathrm{H}^+)^3)$ (Fig. 10) diagrams have been constructed using the SYSTEM module of the computer program THERMOCHEMISTRY (Turnball, 1977) and the thermodynamic data set of Holland & Powell (1998). The diagrams were calculated for the chemical system NKASH, including the following mineral endmembers: quartz, paragonite, kyanite, andalusite, jadeite, albite, K-feldspar, muscovite, corundum, diaspore, nepheline, kalsilite, pyrophyllite and kaolinite. The following electrolytes were also considered: Na^+, K^+, H^+, Al^{3+}. The diagrams have been constructed for four different sets of *P–T* conditions that represent different stages in the metamorphic evolution of the

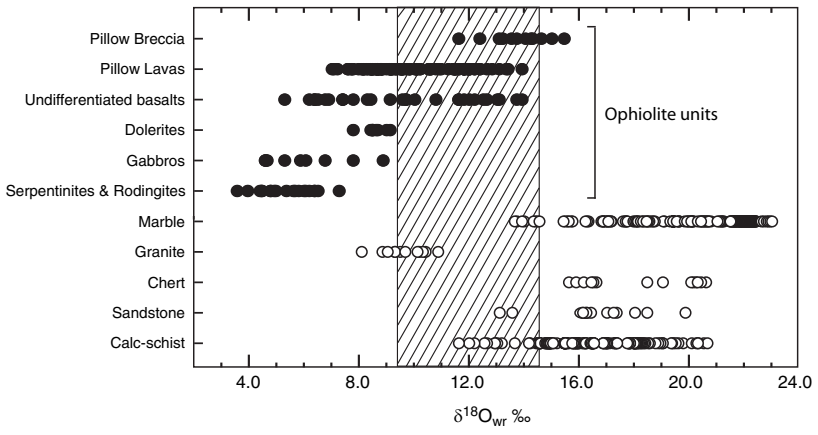

Fig. 8. Oxygen isotope compositions of the major rock types from Alpine Corsica. Data from Miller *et al.* (2001). Shaded region indicates the likely $\delta^{18}O$ composition of the fluid in equilibrium with the albite veins.

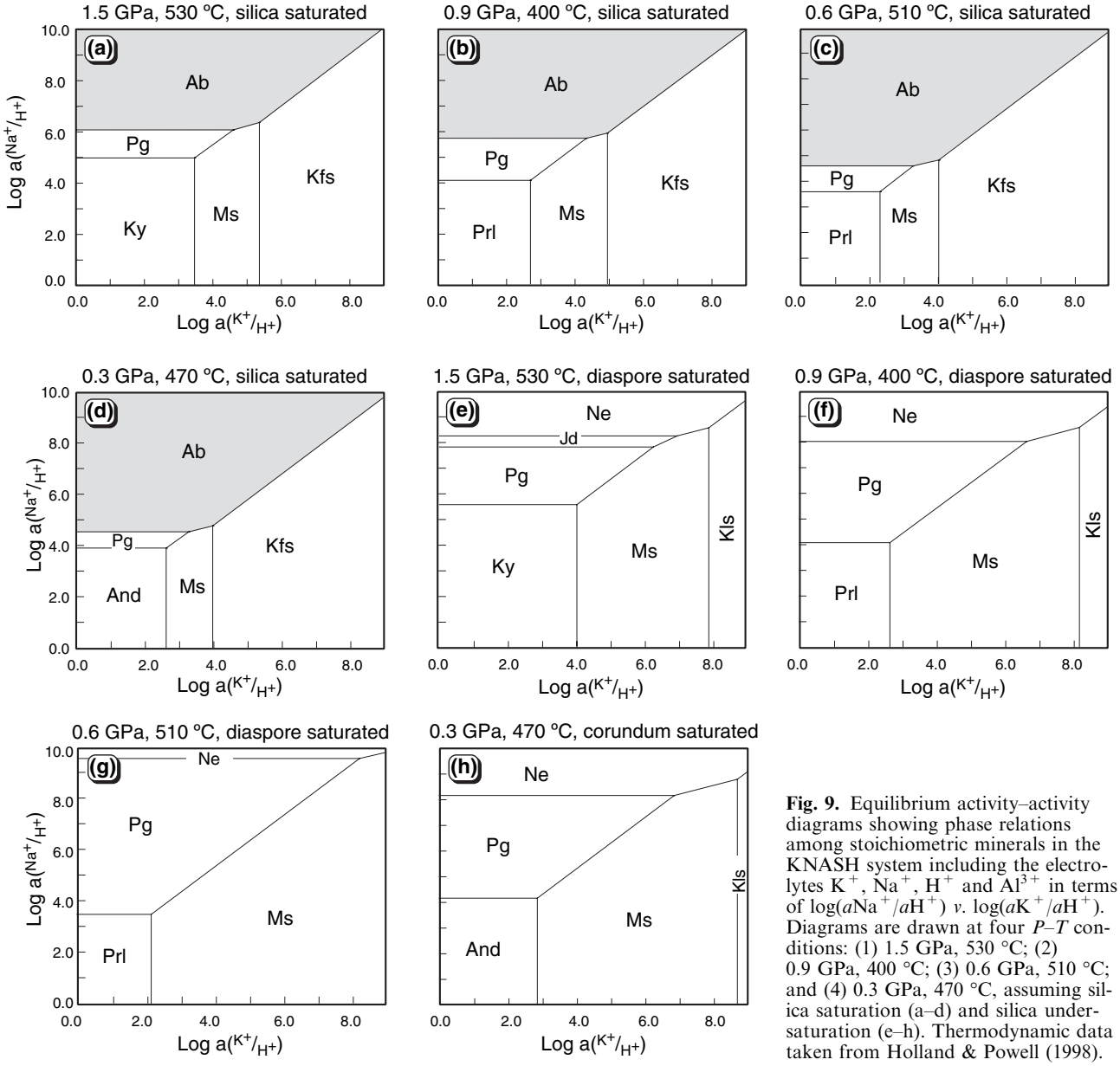

Fig. 9. Equilibrium activity–activity diagrams showing phase relations among stoichiometric minerals in the KNASH system including the electrolytes K^+, Na^+, H^+ and Al^{3+} in terms of $\log(a\mathrm{Na}^+/a\mathrm{H}^+)$ *v.* $\log(a\mathrm{K}^+/a\mathrm{H}^+)$. Diagrams are drawn at four *P–T* conditions: (1) 1.5 GPa, 530 °C; (2) 0.9 GPa, 400 °C; (3) 0.6 GPa, 510 °C; and (4) 0.3 GPa, 470 °C, assuming silica saturation (a–d) and silica undersaturation (e–h). Thermodynamic data taken from Holland & Powell (1998).

Corsican metabasalts: (1) lawsonite–eclogite facies, 1.5 GPa, 530 °C; (2) blueschist facies, 0.9 GPa, 400 °C; (3) regional greenschist facies overprint, 0.6 GPa, 510 °C; and (4) albite vein formation, 0.3 GPa, 470 °C. Manning (1998) discussed in more detail the construction of these types of diagrams for high-pressure metabasaltic rock systems.

Silica saturation

Given that quartz veins are present in high-pressure terranes from eclogite facies (Kerrich, 1988) through to greenschist facies (Cartwright & Buick, 2000) the question of why albite is precipitated into the veins rather than quartz is one that needs to be addressed. The quartz-absent nature of the veins and the alteration haloes combined with the fact that the solubility of albite is comparable to, or exceeds that of quartz at moderate to high pressures (Anderson & Burnham, 1983; Manning, 1998) suggests that the vein-forming fluid may be undersaturated with respect to silica. Figure 9(a–d) illustrates the variation in $\log(a\mathrm{Na}^+/a\mathrm{H}^+)$ *v.* $\log(a\mathrm{K}^+/a\mathrm{H}^+)$ from *P–T* conditions of eclogite facies to albite vein formation on Corsica, assuming silica saturation, whilst Fig. 9(e–f) illustrate changes in the same system assuming silica undersaturation. The principal difference between these two sets of diagrams is that albite is unstable with respect to paragonite and the more Al-rich phase nepheline, in the silica-under-

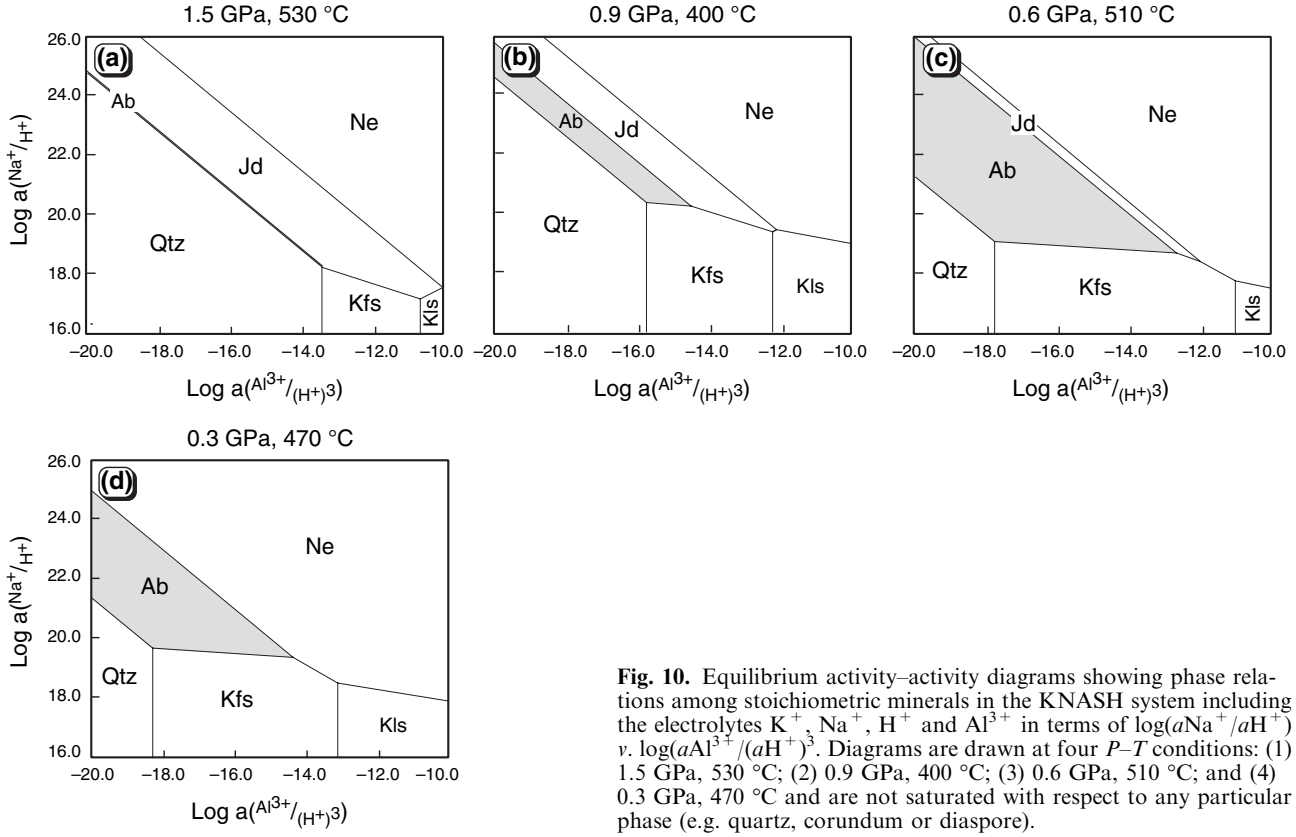

Fig. 10. Equilibrium activity–activity diagrams showing phase relations among stoichiometric minerals in the KNASH system including the electrolytes K^+, Na^+, H^+ and Al^{3+} in terms of $\log(a\mathrm{Na}^+/a\mathrm{H}^+)$ *v.* $\log(a\mathrm{Al}^{3+}/(a\mathrm{H}^+)^3$. Diagrams are drawn at four *P–T* conditions: (1) 1.5 GPa, 530 °C; (2) 0.9 GPa, 400 °C; (3) 0.6 GPa, 510 °C; and (4) 0.3 GPa, 470 °C and are not saturated with respect to any particular phase (e.g. quartz, corundum or diaspore).

saturated system. These diagrams therefore indicate that the fluid from which the albite veins were precipitated was closer to silica saturation than Al-saturation.

Na:K ratios

In the case where the vein-forming fluid is silica-saturated, Fig. 9(a–d) illustrates the influence of the Na:K ratio of the fluid on the stabilization of albite. In $\log(a\mathrm{Na}^+/a\mathrm{H}^+)$ *v.* $\log(a\mathrm{K}^+/a\mathrm{H}^+)$ space, albite and K-feldspar are stable together at the four *P–T* conditions calculated. In order that albite will be stabilized in preference to K-feldspar, Fig. 9(a–d) indicates that the Na:K ratio of the fluid phase needs to be in excess of 1.2. This ratio does not appear to be dependent on pressure or temperature conditions and likely represents a ratio set by the mineralogy and composition of the rocks from which the fluid is derived. This is because the concentration of different elements in a fluid phase is usually buffered by reactions involving minerals containing the elements of interest (Eugster & Baumgartner, 1987; Pokrovskii & Helgeson, 1995). In the case of the Corsican albite veins, the host metabasalts have Na_2O contents of between 1.3 and 5.0 wt%, reflecting the presence of sodic amphibole and pyroxene as well as albite, whilst K_2O contents are generally less than 0.5 wt% reflecting the lack of any significant K-bearing phase. Thus any fluids generated by breakdown of hydrous phases in the hostrocks to the albite veins should have significantly higher concentrations of Na than K and will thus under the right conditions lead to the formation of albite. However, Fig. 9(a–d) indicates that given the right Na:K ratio, albite is stable at all the *P–T* conditions studied. This is clearly not the case in reality, as albite veins do not occur at pressures in excess of around 8 GPa. Thus, although the Na:K ratio is important in the formation of albite veins it does not play a role in the preference for albite vein formation at low pressure over other vein-forming phases.

Solubility and speciation of aluminium

The concentration of aluminium in the fluid phase is strongly dependent on pressure (Manning, 1998) and thus aluminium solubility is likely to play a role in the formation of albite veins. Aluminium has long been considered a relatively immobile element which is contrary to its presence in a wide range of vein minerals including both albite and kyanite, in addition to amphibole and pyroxene. As a result numerous studies have attempted to determine the relative stabilities of various aluminium species including $Al(OH)^{2+}$, $Al(OH)_2^+$, $Al(OH)_3$, $Al(OH)_4^-$ as well as the aluminium

ion Al^{3+} and a range of Al-complexes including $NaAl(OH)_4$ (see review by Pokrovskii & Helgeson, 1995). Although there is some debate as to whether aluminium complexing is required at high-pressures (for example, Anderson, 1995), recent studies have identified both Na and K (Pokrovskii & Helgeson, 1992, 1995) and Si (Salvi *et al.*, 1998) as elements that may form aluminium complexes, and hence increase the solubility of aluminium at moderate to high pressures. However, the types of complexes that aluminium forms depend in part on the pH of the fluid. Manning (1998) found that fluids in equilibrium with basic rocks at high pressures were likely to be basic with pHs in the range 9–9.5 and that the dominant Al species was AlO_2^-. However, other aluminium species such as $Al(OH)_4^-$ (Walther & Woodland, 1993; Anderson, 1995) and $Al(OH)_3$ and Al^{3+} (Woodland & Walther, 1987) have also been postulated as the dominant aluminium species in solution. Clarification of aluminium speciation in high-pressure metamorphic fluids is certainly an important step in assessing the role of aluminium solubility in constraining albite vein formation.

This point can be illustrated by looking at changes in mineral stabilities as a function of the pressure dependence of the concentration of the Al^{3+} species in $\log(a\mathrm{Na}^+/a\mathrm{H}^+)$ *v.* $\log(a\mathrm{Al}^{3+}/(a\mathrm{H}^+)^3)$ space (Fig. 10). These plots show that the concentration of the Al^{3+} species is predicated to be fairly low at all the *P–T* conditions under consideration and probably too low to form albite unless unrealistically large volumes of fluid were involved (and thus indirectly, indicate that other aluminium species must play a role in aluminium transport). Nevertheless, these figures clearly illustrate the interplay between pressure, albite stability and aluminium solubility and speciation. Under eclogite facies conditions of 1.5 GPa and 530 °C (Fig. 10a), albite occupies an extremely restricted $\log(a\mathrm{Na}^+/a\mathrm{H}^+)$ *v.* $\log(a\mathrm{Al}^{3+}/(a\mathrm{H}^+)^3)$ compositional range. The transition from (a) to (d) shows the increase in the stability of albite with respect to quartz and jadeite, consistent with the albite breakdown reaction albite = jadeite + quartz, and represents an increase in the stability of albite by three orders of magnitude during decompression. As the total solubility of aluminium is pressure sensitive (Manning, 1994, 1998), any sudden drop in fluid pressure, for example in response to fracture development is a plausible mechanism for driving albite precipitation in veins at the *P–T* conditions of interest (see below).

P–T conditions and fluid generation during exhumation

Decompression dehydration

The extent and timing of dehydration of the subducting slab depends upon the *P–T* path the slab follows within the subduction zone (Peacock, 1990). Rocks that follow a cold *P–T* path will experience lawsonite–blueschist facies conditions and will potentially contain around 6 wt% H_2O (Hacker, 1996; Bousquet *et al.*, 1997), primarily bound in hydrous minerals such as lawsonite, glaucophane and clinozoisite, as is the case for the Corsican metabasalts. At higher grades, where lawsonite breakdown occurs on the prograde metamorphic path, other hydrous minerals such as zoisite, clinozoisite, white mica and amphibole will be formed. In both cases these minerals may be an important source of fluid during decompression and exhumation of high-pressure terranes. Numerous studies have investigated the mineral reactions that occur at the transition from the blueschist to greenschist facies (e.g. Carson *et al.*, 1990; Will *et al.*, 1990, 1998; Gómez-Pugnaire *et al.*, 1997) and it is not the intention of this study to undertake a detailed study of the petrogenetic evolution of such phases. However, some consideration of possible reactions for generating the albite vein forming fluid is appropriate in light of the findings of this study so far. The influx of externally derived fluids as a mechanism for driving mineral reactions and retrogression of blueschist and eclogite facies assemblages is not considered appropriate for the rocks in this study on the basis of the stable isotope data. Thus the fluids must have been generated internally, something that is considered feasible in the case of these rocks owing to the relative abundance of lawsonite which contains up to 11 wt% H_2O.

Lawsonite is a high-pressure, low-temperature mineral whose maximum temperature stability in the *P–T* region of interest here, is governed by the breakdown reaction: lawsonite = kyanite + clinozoisite + quartz + H_2O. In the Western Alps this reaction is normally intersected on the prograde path such that lawsonite is only preserved as pseudomorphs or as inclusions in garnet (e.g. Barnicoat & Fry, 1986). However, for the Corsican metabasalts, the presence of abundant lawsonite at both eclogite and blueschist facies indicates that it remained stable during at least the early stages of decompression. The relationship between lawsonite stability and high-pressure metamorphism on Corsica is complicated as some of the estimated *P–T* conditions are in fact well in excess of the theoretical stability of lawsonite. Figure 11 shows the position of the maximum stability of lawsonite and the *P–T* conditions estimated for Alpine Corsica from various studies. Estimates of the *P–T* conditions of the eclogite facies event are usually higher than the maximum stability of lawsonite even though lawsonite is cited as part of the eclogitic assemblage. Similarly some of the blueschist facies *P–T* conditions are also higher than the maximum stability of lawsonite. Resolving this discrepancy is beyond the scope of this paper but the absence of quartz in the metabasalts at any metamorphic grade suggests that the lawsonite breakdown reaction was not 'seen' by the Corsican metabasalts as greenschist facies conditions are clearly in excess of this terminal reaction and greenschist facies rocks contain neither lawsonite nor quartz. For the

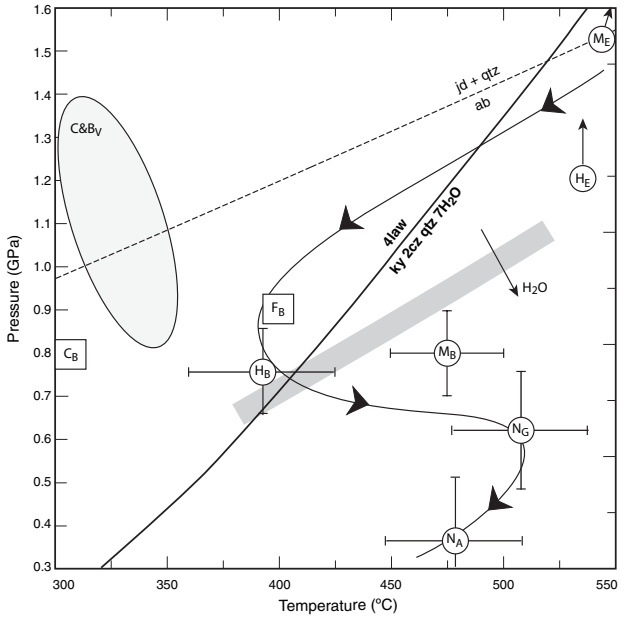

Fig. 11. Alpine Corsica *P–T* conditions for the eclogite and blueschist facies metamorphism from the literature and for the greenschist facies retrogression and albite vein formation calculated in this study. Positions of the terminal reactions for albite (dashed line) and lawsonite (solid line) stability calculated using the Holland & Powell (1998) data set. Abbreviations as follows: Eclogite facies *P–T* conditions from: H_E, Harris (1984); M_E, Malavielle *et al.* (1998); Blueschist facies *P–T* conditions from: C_B, Caron *et al.* (1981); H_B, Harris (1984); F_B, Fournier *et al.* (1991); M_B, Malavielle *et al.* (1998); N_G, greenschist facies *P–T* conditions from this study; and N_A, the *P–T* conditions of albite vein formation from this study. Shaded grey field labelled C&BV indicates the range of *P–T* conditions indicated for fluid generation forming quartz and calcite veins in the Schistes Lustrés by Cartwright & Buick (2000). Shaded grey line indicates the general gradient of fluid generating reactions given in various studies of high-pressure metabasaltic rocks with H_2O being generated on the low-*P*/High-*T* side of the line (e.g. Guiraud *et al.*, 2001; Fitzherbert *et al.*, 2005).

Corsican metabasalts the transition from eclogite to blueschist *P–T* conditions is accompanied by an increase in H_2O contents of around 2 wt%, from 3.2 to 5.3 wt% (taking LOI as a proxy for H_2O in carbonate absent rocks where wt% CO_2 is less than 0.15; Miller, unpublished data). However, the greenschist facies assemblages contain on average 3.2 wt% H_2O similar to the eclogite facies rocks. Thus the bulk of lawsonite breakdown occurs during the transition from blueschist to greenschist facies conditions and probably involves reactions such as glaucophane + lawsonite + garnet = albite + clinozoisite + clinoamphibole + H_2O or Na-pyroxene + glaucophane + lawsonite = chlorite + clinozoisite + albite + H_2O. Both these reactions generate substantial volumes of H_2O on the low-*P*–high-*T* side of the reaction going towards the greenschist facies (Fig. 11), which if retained in the rocks, could provide a fluid source for the formation of the albite veins.

Hydro-fracturing during decompression

The generation of fluid during decompression, as discussed above, may provide the mechanism that drives the formation of fractures into which albite is precipitated. Barnicoat (1988) examined the development of hydraulic fracturing in the Zermatt-Saas albite veins by investigating the relationship between the P_{fluid}/P_{load} using Sibson's (1981) analysis of simultaneous shear failure and hydraulic fracture. However, this analysis considered isothermal, isobaric conditions and did not take into account the changing physical properties of water as the rocks decompress. During decompression the density of fluid decreases (Brown & Lamb, 1989) equating to an increase in fluid volume that can promote hydro-fracturing. However, this will only be the case if the change in fluid density is greater than the change in the rock density. Figure 12 shows the change in the density of H_2O during decompression and indicates a decrease in density from *c.* 1.1 g cm^{-3} to *c.* 0.84 g cm^{-3}, which equates to an overall volume increase of *c.* 31%. However, the greatest change in the density of H_2O occurs during the transition from blueschist to vein formation *P–T* conditions. This is the most likely stage at which lawsonite breakdown occurs on Corsica, as the blueschist assemblage is lawsonite-bearing whilst the greenschist assemblage is not. This transition accounts for a 25% increase in the

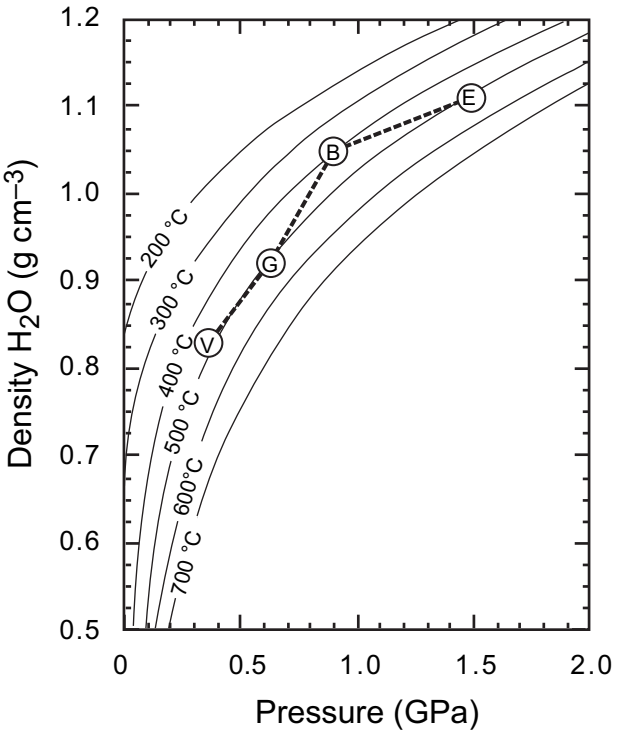

Fig. 12. Changes in the density of H_2O as a function of pressure and temperature as rocks are exhumed from high pressures (constructed using the Holland & Powell (1998) data set). V, vein; E, eclogite; B, blueschist; G, greenschist.

volume of H_2O. However, Bousquet *et al.* (1997) calculated using equilibrium mineral assemblages in gabbroic and andesitic rock compositions, that the transition from blueschist to vein-formation P–T conditions results in a rock density decrease of only 0.16 g cm^{-3} (Fig. 3), which equates to a volume increase of approximately 5%. Therefore, because the volume increase of the fluid is much greater than that of the rocks, fluid generation during decompression is likely to induce hydraulic fracturing (Beach, 1977; Yardley, 1983; Boullier *et al.*, 1994). The development of fractures will immediately lead to a reduction in hydraulic head. However, in order to drive fluid from the fracture out into the wallrocks and generate an alteration halo, the hydraulic head needs to be increased. Barnicoat (1988) postulated that an increase in hydraulic head may occur because P_{fluid} becomes insufficient to hold open the fracture, or because a partial choke develops within the vein leading to P_{fluid} exceeding P_{load}. Reactions that form the alteration halo mineralogy potentially take place at lower P–T conditions than those that generate the H_2O involved in vein-formation and could be the result of fluid cycling around the developing vein as a result of oscillations in P_{fluid}, which may explain the lack of isotopic equilibration and mass balance between the veins and their hostrocks. The rapid opening of hydrofractures may also promote very rapid precipitation of albite because of sudden decreases in pressure and hence the solubility of chemical components in the fluid phase. Such a situation is commonly cited for the formation of quartz veins (Henderson & McCaig, 1996; Sibson & Scott, 1998; Bons, 2001).

CONCLUSIONS

While albite veins are common in many high-pressure terranes, the processes that lead to their formation are complex. Using petrography, mineral chemistry, stable isotope and whole-rock geochemistry, we have investigated the formation of albite veins from the Alpine ophiolite complex of Corsica. Stable isotope data indicate that the fluids involved in the formation of the albite veins were derived from within the ophiolite and most likely from within the metabasaltic units of the ophiolite. However, fluid flow probably occurred on a greater than outcrop scale. This is similar to the method of vein formation proposed for quartz–calcite veins in the overlying Schistes Lustrés (Cartwright & Buick, 2000). This implies that the rocks from which the albite veins formed did not completely dehydrate during prograde high-pressure subduction zone metamorphism. The breakdown of hydrous high-pressure minerals such as lawsonite during decompression and exhumation of the ophiolite complex may provide an important fluid source for the formation of albite veins. From this data we propose the following model for the formation of albite veins:

1. Initial hydration and Na enrichment of the rocks whilst they are still in an oceanic environment.
2. Incorporation of water within hydrous high-pressure minerals as the rocks are subducted to greater and greater depths.
3. Decompression and exhumation subsequent to high-pressure metamorphism during which retrograde dehydration reactions are intersected.
4. Water-rich fluids generated during exhumation are initially dispersed as a grain-boundary fluid.
5. As rocks continue to decompress, the fluid regime changes from grain-boundary hosted to fracture controlled. This transition may be favoured by the change in the density of water during decompression.
6. Precipitation of albite into fractures via a free-fluid phase is probably controlled by the solubility of aluminium.
7. Fluid migration into the vein wallrock to form the vein alteration halo may have been driven by excess hydraulic head in response to P_{fluid} exceeding P_{load}. This situation can be forced by the deposition of albite in the vein causing a choke to develop.
8. Late fluid flow driving localized precipitation of calcite in existing fracture systems.

The most significant finding of this study is that the veins are internally derived within the metabasalts, although they represent flow systems on a larger than outcrop scale. This is contrary to the study of Barnicoat (1988), which concluded that the fluids required for albite vein formation must have been externally derived. The concept of internally derived fluids for vein formation in high-pressure terranes goes against the concept of all metabasic eclogites being 'dry' rocks. However, there have now been several studies that have postulated that the development of hydrous high-pressure phases such as lawsonite, phengite, paragonite, chloritoid, carpholite and glaucophane may play an important role in the storage of water at depth in the crust (see review by Schreyer, 1995). In addition, quartz–kyanite veins, considered to have formed at the peak of metamorphism, have been documented from several high-pressure suites including the Lepontine Alps (Kerrich, 1988) and the Zermatt-Saas Zone (Cartwright & Barnicoat, 1999). A potential test of this hypothesis is to investigate the presence and abundance of veins in a variety of high-pressure terranes to see if veining is more common in terranes that have undergone a lesser degree of dehydration. Field observations suggest that at least for Alpine Corsica, veining is more abundant in the low-temperature lawsonite-bearing Corsican rocks, indicating that the formation of late-stage veining is dependent on the prior P–T history of the high-pressure rock sequences.

ACKNOWLEDGEMENTS

This research was supported by ARC grant A39531124 to I. Cartwright and I.S. Buick. J.A. Miller acknowledges the support of an Australian Postgraduate

Award and Monash University Overseas Study Grant and Conference Support Grants. We thank M. Jane and M. Yanni for assistance with the running of stable isotopes. J. Brugger and D.C. McPhail helped with the running of the program SYSTEM used to construct Figs 9 and 10. E. Condliffe assisted with electron microprobe analyses at the University of Leeds and we are grateful to the staff of the CEMMSA facility for assistance with the electron microprobe facilities at the University of Adelaide. Discussions with I.S. Buick, M. Krabbendam and D.C. McPhail helped to clarify some of the ideas presented in this manuscript. The manuscript was improved by constructive reviews from D. Whitney, A. Baker, A. Barnicoat and P. Hoskin.

REFERENCES

Agard, P., Goffé, B., Touret, J.L.R. & Vidal, O., 2000. Retrograde mineral and fluid evolution in high-pressure metapelites (Schistes lustrés unit, Western Alps). *Contributions to Mineralogy and Petrology*, **140,** 296–315.

Anderson, G.M., 1995. Is there alkali-aluminum complexing at high temperatures and pressures. *Geochimica et Cosmochimica Acta*, **59,** 2155–2161.

Anderson, G.M. & Burnham, C.W., 1983. Feldspar solubility and the transport of aluminium under metamorphic conditions. *American Journal of Science*, **238A,** 283–297.

Barnicoat, A.C., 1988. The mechanism of veining and retrograde alteration of Alpine eclogites. *Journal of Metamorphic Geology*, **6,** 545–558.

Barnicoat, A.C. & Fry, N., 1986. High-pressure metamorphism of the Zermatt-Saas ophiolite zone, Switzerland. *Journal of the Geological Society, London*, **143,** 603–618.

Barrientos, X., 1991. Petrology of Coexisting Blueschist and Greenschists, Ile de Groix, France: Implications for Preservation of Blueschists. PhD Thesis, Harvard University, Cambridge, MA.

Barrientos, X. & Selverstone, J., 1993. Infiltration vs thermal overprinting of epidote blueschists, Ile de Groix, France. *Geology*, **21,** 69–72.

Beach, A., 1977. Vein arrays, hydraulic fractures and pressure solution structures in a deformed flysch sequence, SW England. *Tectonophysics*, **40,** 201–225.

Bebout, G.E. & Barton, M.D., 1989. Fluid flow and metasomatism in a subduction zone hydrothermal system, Catalina Schist Terrane, California. *Geology*, **17,** 976–980.

Bebout, G.E. & Barton, M.D., 1993. Metasomatism during subduction: products and possible paths in the Catalina Schist, California. *Chemical Geology*, **108,** 61–92.

Bons, P.D., 2001. The formation of large quartz veins by rapid ascent of fluids in mobile hydrofractures. *Tectonophysics*, **336,** 1–17.

Boullier, A.-M., Charoy, B. & Pollard, P.J., 1994. Fluctuations in porosity and fluid pressure during hydrothermal events: textural evidence in the Emuford District, Australia. *Journal of Structural Geology*, **16,** 1417–1429.

Bousquet, R., Goffé, B., Henry, P., Le Pichon, X. & Chopin, C., 1997. Kinematic, thermal and petrological model of the Central Alps: Lepontine metamorphism in the upper crust and eclogitisation of the lower crust. *Tectonophysics*, **273,** 105–127.

Bowtell, S.A., Cliff, R.A. & Barnicoat, A.C., 1994. Sm–Nd isotopic evidence on the age of eclogitisation in the Zermatt-Saas ophiolite. *Journal of Metamorphic Geology*, **12,** 187–196.

Brown, P.E. & Lamb, W.M., 1989. P–V–T properties of fluids in the system $H_2O \pm CO_2 \pm$ NaCl: new graphical presentations and implications for fluid inclusion studies. *Geochimica et Cosmochimica Acta*, **53,** 1209–1221.

Brunet, C., Monié, P. & Jolivet, L., 1997. Geodynamic evolution of Alpine Corsica based on new $^{40}Ar/^{39}Ar$ data. *Terra Abstracts*, **9,** 493.

Brunsmann, A., Franz, G., Erzinger, J. & Landwehr, D., 2000. Zoisite and clinozoisite-segregations in metabasites (Tauern Window, Austria) as evidence for high-pressure fluid–rock interaction. *Journal of Metamorphic Geology*, **18,** 1–21.

Caron, J-M, 1994. Metamorphism and deformation in Alpine Corsica. *Schweizerische Mineralogische Petrogrographische Mitteilungen*, **74,** 105–114.

Caron, J-M., Kienast, J.R. & Triboulet, C., 1981. High-pressure–low-temperature metamorphism and polyphase alpine deformation at Sant' Andrea Di Cotone (Eastern Corsica, France). *Tectonophysics*, **78,** 419–451.

Carpena, J., Mailhé, D., Naeser, C.W. & Poupeau, G., 1979. Sur la datation par traces de fission d'une phase tectonic d'âge éocène superieur en Corse. *C.R. Academie du Sciences, Paris*, **289,** 829–832.

Carson, C.J., Clarke, G.L. & Powell, R., 1990. Hydration of eclogite, Pam Peninsula, New Caledonia. *Journal of Metamorphic Geology*, **18,** 79–90.

Cartwright, I. & Barnicoat, A.C., 1999. Stable isotope geochemistry of alpine ophiolites: a window to ocean floor hydrothermal alteration and constraints on fluid–rock interaction during high-pressure metamorphism. *International Journal of Earth Sciences*, **88,** 219–235.

Cartwright, I. & Buick, I.S., 2000. Fluid generation, vein formation, and the degree of fluid–rock interaction during decompression of high-pressure terranes: the Schists Lustrés, Alpine Corsica, France. *Journal of Metamorphic Geology*, **18,** 607–624.

Clayton, R.N. & Mayeda, T.K., 1963. The use of bromine pentafluoride in the extraction of oxygen from oxides and silicates for isotopic analysis. *Geochimica et Cosmochimica Acta*, **27,** 43–52.

Clayton, R.N., Goldsmith, J.R. & Mayeda, T.K., 1989. Oxygen isotope fractionation in quartz, albite, anorthite and calcite. *Geochimica et Cosmochimica Acta*, **39,** 1197–1201.

Cliff, R.A., Barnicoat, A.C. & Inger, S., 1997. Early Tertiary eclogite facies metamorphism in the Monviso Ophiolite. *Journal of Metamorphic Geology*, **16,** 447–455.

Coward, M.P. & Dietrich, D., 1989. Alpine tectonics – an overview. In: *Alpine Tectonics* (eds Coward, M.P. & Dietrich, D.), *Geological Society of London, Special Publication*, **45,** 1–29.

Daniel, J.M., Jolivet, L., Goffé, B. & Poinssot, C., 1996. Crustal-scale strain partitioning: footwall deformation below the Alpine Oligo-Miocene detachment of Corsica. *Journal of Structural Geology*, **18,** 41–49.

Eugster, H.P. & Baumgartner, L., 1987. Mineral solubilities and speciation in supercritical metamorphic fluids. In: *Thermodynamic Modelling of Geological Materials: Minerals, Fluids and Melts* (eds Carmichael, I.S.E. & Eugster, H.P.). *Mineralogical Society of America. Reviews in Mineralogy*, **17,** 367–404.

Ferry, J.M. & Dipple, G.M., 1991. Fluid flow, mineral reactions and metasomatism. *Geology*, **19,** 211–214.

Fisher, D. & Byrne, T., 1990. The character and distribution of mineralised fractures in the Kodiak Formation, Alaska: implications for fluid flow in an underthrust sequence. *Journal of Geophysical Research*, **96,** 9069–9080.

Fitzherbert, J.A., Clarke, G.L. & Powell, R., 2005. Preferential retrogression of high-P metasediments and the preservation of blueschist to eclogite facies metabasite during exhumation, Diahot terrane, NE New Caledonia. *Lithos*, **83,** 67–96.

Fournier, M., Jolivet, L., Goffé, B. & Dubois, R., 1991. Alpine Corsica metamorphic core complex. *Tectonics*, **10,** 1173–1186.

Franz, A. & Liebscher, G., 2004. Epidotes. *Reviews in Mineralogy and Geochemistry*, **56,** 1–82.

Friedman, I. & O'Neil, J.R., 1977. Compilation of stable isotope fractionation factors of geochemical interest. *Data of Geochemistry, U.S. Geological Survey Professional Paper*, 440-KK.

Ganor, J., Matthews, A. & Schliestedt, M., 1994. Post-metamorphic low $\delta^{13}C$ calcite in the Cycladic complex (Greece) and their implications for modelling fluid infiltration processes using carbon isotope compositions. *European Journal of Mineralogy*, **6,** 365–379.

Garlick, G.D., 1966. Oxygen isotope fractionation in igneous rocks. *Earth and Planetary Science Letters*, **1,** 361–368.

Getty, S.R. & Selverstone, J., 1994. Stable isotopic and trace element evidence for restricted fluid migration in 2GPa eclogites. *Journal of Metamorphic Geology*, **12,** 747–760.

Gómez-Pugnaire, M.T., Karsten, L. & López Sáchez-Vizcaíno, V., 1997. Phase relationships and *P–T* conditions of coexisting eclogite-blueschist and their transformation to greenschist-facies rocks in the Nerkau Complex (Northern Urals). *Tectonophysics*, **276,** 195–216.

Guiraud, M., Powell, R. & Rebay, G., 2001. H_2O in metamorphism and unexpected behaviour in the preservation of metamorphic mineral assemblages. *Journal of Metamorphic Geology*, **19,** 445–454.

Hacker, B.R., 1996. Eclogite formation and the rheology, buoyancy, seismicity, and H_2O content of oceanic crust. In: *Subduction: Top to Bottom* (eds Bebout, G.E., Scholl, D.W., Kirby, S.H. & Platt, J.P.). *American Geophysical Union Monograph*, **96,** 337–346.

Harris, L.B., 1984. *Déformations et déplacements dans la chaîne alpine: l'exemple des Schistes lustrés du Cap Corse*, 307 pp. Thèse de 3^e cycle, Rennes.

Henderson, I.H.C. & McCaig, A.M., 1996. Fluid pressure and salinity variations in shear zone-related veins, central Pyrenees, France: implications for the fault-valve model. *Tectonophysics*, **262,** 321–348.

Henry, C., Burkhard, M. & Goffé, B., 1996. Evolution of syn-metamorphic veins and their wallrocks through a Western Alps transect: no evidence for large-scale fluid flow. Stable isotope, major and trace-element systematics. *Chemical Geology*, **127,** 81–109.

Hoefs, J., 1997. *Stable Isotope Geochemistry*. Springer, Berlin.

Holland, T.J.B. & Blundy, J., 1994. Non-ideal interactions in calcic amphiboles and their bearing on amphibole plagioclase thermometry. *Contributions to Mineralogy and Petrology*, **116,** 433–447.

Holland, T.J.B. & Powell, R., 1998. An internally consistent thermodynamic data set for phases of petrological interest. *Journal of Metamorphic Geology*, **16,** 309–343.

Kerrich, D.M., 1988. Al_2SiO_5-bearing segregations in the Lepontine Alps, Switzerland: aluminium solubility in metapelites. *Geology*, **16,** 636–640.

van der Klauw, S.N.G.C., Reinecke, T. & Stockert, B., 1997. Exhumation of ultrahigh-pressure metamorphic oceanic crust from Lago di Cignana, Piemontese zone, Western Alps: the structural record in metabasites. *Lithos*, **41,** 79–102.

Kretz, R. 1983. Symbols for rock-forming minerals. *American Mineralogist*, **68,** 277–279.

Lahondère, D., 1991. *Les schistes bleu et les éclogites à lawsonite des unités continentales et océaniques de la Corse alpine: nouvellees données pétrologiques et structurales*. Thèse de doctorat, Montpellier, France.

Lahondère, D. & Guerrot, C. 1997. Datation Sm-Nd du métamorphisme écolgitique en Corse alpine: un argument pour l'existence an Crétacé supérieur d'une zone de subduction active localisée sous le bloc corso-sarde. *Géologie de la France*, **3,** 3–11.

Malavielle, J., Chemenda, A. & Larroque, C., 1998. Evolutionary model for Alpine Corsica: mechanism for ophiolite emplacement and exhumation of high-pressure rocks. *Terra Nova*, **10,** 317–322.

Maluski, H., 1977. *Application de la méthode* ^{40}Ar–^{39}Ar aux minéraux des roches cristallines perturbées par des événements thermiques et tectoniques en Corse, 113 pp. Thèse d'Etat, Montpellier, France.

Manning, C.E., 1994. Experimental determination of the solubilities of quartz, kyanite, and corundum in H_2O in the lower crust and upper mantle. *Mineralogical Magazine*, **58A,** 555–556.

Manning, C.E., 1998. Fluid composition at the blueschist–eclogite transition in the model system Na_2O–MgO–Al_2O_3–SiO_2–H_2O–HCl. *Schweizerische Mineralogische Petrographische Mitteilungen*, **78,** 225–242.

McCrea, J.M., 1950. On the isotope chemistry of carbonates and a palaeo-temperature scale. *Journal of Chemical Physics*, **18,** 849–857.

Miller, J.A., Cartwright, I. & Barnicoat, A.C., 1998. The formation of albite veins in high-pressure terranes: examples from Corsica, France and Zermatt-Saas, Switzerland. In: *Proceedings of the 9th International Symposium on Water–Rock Interaction*, pp. 789–792. Balkema, Rotterdam.

Miller, J.A., Cartwright, I., Buick, I.C. & Barnicoat, A.C, 2001. An O-isotope profile through the HP–LT Corsican ophiolite, France and its implications for fluid flow during subduction. *Chemical Geology*, **178,** 43–69.

Nelson, B.K., 1991. Sediment-derived fluids in subduction zones: isotopic evidence from veins in blueschist and eclogite of the Franciscan Complex, California. *Geology*, **19,** 1033–1036.

Oliver, N.H., 1996. Review and classification of structural controls on fluid flow during regional metamorphism. *Journal of Structural Geology*, **14,** 477–492.

Oliver, N.H.S. & Bons, P.D., 2001. Mechanisms of fluid flow and fluid rock interaction in fossil metamorphic hydrothermal systems inferred from vein-wallrock patterns, geometry and microstructure. *Geofluids*, **1,** 137–162.

Peacock, S.M., 1990. Fluid processes in subduction zones. *Science*, **248,** 329–337.

Pequignot, G. & Potdevin, J.L., 1984. *Metamorphisme et tectonique dans les Schistes lustrés a l'Est de Corte (Corse)*, 289 pp. Thèse de 3^e cycle, Lyon.

Philippot, P. & Rumble, D. 2000. Fluid–rock interactions in HP and UHP rocks. *International Geology Review*, **42,** 312–327.

Philippot, P. & Selverstone, J., 1991. Trace element rich brines in eclogite veins: implications for fluid composition and transport during subduction. *Contributions to Mineralogy and Petrology*, **106,** 417–430.

Pognante, U., 1991. Petrologic constraints for the eclogite- and blueschist-facies metamorphism and P–T–t paths in the Western Alps. *Journal of Metamorphic Geology*, **9,** 5–19.

Pokrovskii, V.A. & Helgeson, H.C., 1992. Calculation of the thermodynamic properties of mononuclear aqueous Al species in the system Al_2O_3–H_2O–NaCl at temperatures to 1000 °C and pressures to 5 kb. *Proceedings of the 7th International Symposium on Water–Rock Interaction*, pp. 1021–1024. Balkema, Rotterdam.

Pokrovskii, V.A. & Helgeson, H.C., 1995. Thermodynamic properties of aqueous species and the solubility of minerals at high pressures and temperatures: the system Al_2O_3–H_2O–NaCl. *American Journal of Science*, **295,** 1255–1342.

Rubatto, D., Gebauer, D. & Fanning, M., 1998. Jurassic formation and Eocene subduction of the Zermatt-Saas-Fee ophiolites: implications for the geodynamic evolution of the Central and Western Alps. *Contributions to Mineralogy and Petrology*, **132,** 269–287.

Salvi, S., Pokrovski, G. & Schott, J., 1998. Experimental investigation of aluminum-silica aqueous complexing at 300 °C. *Chemical Geology*, **151,** 51–67.

Schreyer, W., 1995. Ultradeep metamorphic rocks: the retrospective viewpoint. *Journal of Geophysical Research*, **100,** 8353–8366.

Selverstone, J., Morteani, G. & Staude, J.M., 1991. Fluid channelling during ductile shearing: transformation of granodiorite into aluminous schist in the Tauern Window, eastern Alps. *Journal of Metamorphic Geology*, **9,** 419–431.

Selverstone, J., Franz, G., Thomas, S. & Getty, S., 1992. Fluid variability in 2 GPa eclogites as an indicator of fluid behaviour during subduction. *Contributions to Mineralogy and Petrology*, **112,** 341–357.

Sibson, R.H., 1981. Controls on low-stress hydro-fracture dilatancy in thrust, wrench and normal fault terrains. *Nature*, **289,** 665–667.

Sibson, R.H. & Scott, J., 1998. Stress/fault controls on the containment and release of overpressured fluids: examples from gold-quartz vein systems in Juneau Alaska, Victoria Australia and Otago New Zealand. *Ore Geology Reviews*, **13,** 293–306.

Slater, D.J., Yardley, B.W.D., Spiro, B. & Knipe, R.J., 1994. Incipient metamorphism and deformation in the Variscides of SW Dyfed, Wales: first steps towards isotopic equilibrium. *Journal of Metamorphic Geology*, **12,** 237–248.

Thomas, S., 1990. Segregations and veins in eclogite facies rocks from the Tauern Window, Austria: mineralogy and fluid inclusions. *Geological Society of America Abstracts with Program*, **22,** A257.

Thomas, S., 1991. Zur Kluftbildung in Gesteinen der Eklogitzone (Hohe Tauern, Österreich). *Mitteilungen der Oesterreichischen Geologischen Gesellschaft*, **81,** 189–218.

Turnball, A.G., 1977. A general computer program for the calculation and plotting of thermodynamic stability diagrams. *AusIMM, Extractive Metallurgy Symposium*, Sydney, 10 pp.

Walther, J.V. & Woodland, A.B., 1993. Experimental determination and interpretation of the solubility of the assemblage microcline, muscovite, quartz in supercritical H_2O. *Geochimica et Cosmochimica Acta*, **57,** 2431–2439.

Warburton, J., 1986. The ophiolite-bearing Schistes Lustrés nappe in Alpine Corsica: a model for the emplacement of ophiolites that have suffered HP/LT metamorphism. *Geological Society of America Memoir*, **164,** 313–331.

Waters, C.N., 1989. The metamorphic evolution of the Schistes lustrés ophiolite, Cap Corse, Corsica. *Geological Society, London, Special Publication*, **43,** 557–562.

Waters, C.N., 1990. The Cenozoic tectonic evolution of Alpine Corsica. *Journal of the Geological Society of London*, **147,** 811–824.

Widmer, T.W. & Thompson, A.B., 2001. Local origin of high pressure vein material in eclogite facies rocks of the Zermatt-Saas Zone, Switzerland. *American Journal of Science*, **301,** 627–656.

Will, T., Powell, R., Holland, T.J.B. & Guiraud, M., 1990. Calculated greenschist facies mineral equilibria in the system $CaO–FeO–MgO–Al_2O_3–SiO_2–CO_2–H_2O$. *Contributions to Mineralogy and Petrology*, **104,** 353–368.

Will, T., Okrusch, M., Schmädicke, E. & Chen, G., 1998. Phase relations in the greenschist–blueschist–amphibolite–eclogite facies in the system $Na_2O–CaO–FeO–MgO–Al_2O_3–SiO_2–H_2O$ (NCFMASH), with application to metamorphic rocks from Samos, Greece. *Journal of Metamorphic Geology*, **132,** 85–102.

Wood, B.J. & Walther, J.V., 1986. Fluid flow during metamorphism and its implications for fluid–rock ratios. In: *Fluid–Rock Interactions During Metamorphism* (eds J.V. Walther & B.J. Wood), pp. 89–108. Springer-Verlag, New York.

Woodland, A.B. & Walther, J.V., 1987. Experimental determination of the solubility of the assemblage paragonite, albite, and quartz in supercritical H_2O. *Geochimica et Cosmochimica Acta*, **51,** 365–372.

Yardley, B.W.D., 1983. Quartz veins and devolatilisation during metamorphism. *Journal of the Geological Society, London*, **140,** 657–663.

Yardley, B.W.D. & Bottrell, S.H., 1992. Silica mobility and fluid movement during metamorphism of the Connemara schists, Ireland. *Journal of Metamorphic Geology*, **10,** 453–464.

Received 6 November 2005; revision accepted 6 March 2006.